# Synthesis and MAO Activity of a Series of Benzimidazolyl and Indazolyl Prodrugs

By

Aaron L. Downey

Thesis submitted to the faculty of Virginia Polytechnic Institute and State University in partial fulfillment of the requirements for the degree of

MASTER OF SCIENCE
IN
CHEMISTRY

Dr. Neal Castagnoli, Chairman
Dr. Richard D. Gandour
Dr. James M. Tanko

October 27, 2006

Blacksburg, VA

Keywords: Neuroprotection, Monoamine oxidase, Prodrugs

# Synthesis and MAO Activity of a Series of Benzimidazolyl and Indazolyl Prodrugs

By

Aaron L. Downey

Dr. Neal Castagnoli, Jr., Chairman

## Abstract

Parkinson's disease (PD) is a chronic, progressive disorder of the central nervous system that affects approximately 1.5 million Americans. One of the principal pathological features of PD is dopamine deficiency in the substantia nigra of the brain. A key enzyme that has been associated with the neurodegeneration seen in PD is monoamine oxidase-B (MAO-B). Several inhibitors of this enzyme have resulted in neuroprotection in the mouse model of PD. One such compound is 7-nitroindazole (**1**).

This thesis describes the synthesis and MAO activity of several indazolyl and benzimidazolyl prodrugs that are designed to release an enzyme inhibitor in the affected brain area. These studies have provided information regarding the nucleophilic aromatic substitutions of the ambident nucleophiles under consideration. We have also discovered a compound that releases the enzyme inhibitor upon bioactivation by MAO. These results as well as a MPTP mouse study with the aforementioned compound are detailed within.

# Acknowledgements

I would like to express my deepest thanks and sincere appreciation to Dr. Neal Castagnoli Jr. for his guidance, limitless patience, and continuous support. Without him, none of this would be possible. Dr. Castagnoli provided me with an excellent environment to grow as a chemist and as an individual. It is my hope to one day have such an influence on a person.

I would also like to thank the current and former members of the Castagnoli research group, Mrs. Kay Castagnoli, Dr. Philippe Bissel, Mr. Anthony Miller, Ms. Marina Spanos, Ms. Xiaohua Wu, Dr. Ashraf Khalil, Ms. Rachel Piggott, and Dr. Kazuo Igarashi for all of their efforts in helping me on various projects during my research.

I also wish to thank the Chemistry Department at Virginia Polytechnic Institute and State University for funding in the form of teaching assistantships and the Harvey W. Peters Research Center for Parkinson's Disease and Disorders of the Central Nervous System for supporting me as a research assistant during my time as a graduate student.

# Table of Contents

# List of Figures

# List of Schemes

# 1.0 Introduction

The work described in this thesis represents a continuation of studies initiated by Emre Isin on the enzyme inhibitor properties of 7-nitroindazole [7-NI (**1**)].[1] Of special interest was the observation that **1** inhibited both neuronal nitric oxide synthase (nNOS) and monoamine oxidase (MAO), two enzyme systems that may contribute to neurodegenerative processes involved in the development of Parkinson's disease (PD). Isin's studies focused mainly on MAO. Isin synthesized a prodrug (**72**) of 7-NI that was designed to release the active dual enzyme inhibitor upon metabolic activation by MAO. He also examined the MAO-B inhibiting properties of 5- and 6-nitroindazole. The details and rationale behind these studies are described below.

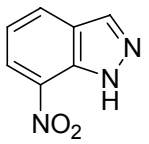


**1**

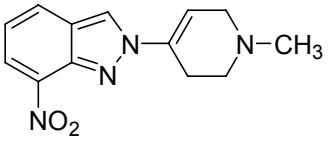


**72**

## 1.1 Parkinson's Disease (PD)

PD is a neurodegenerative disorder whose characteristics include tremor, bradykinesia, rigidity, postural instability, and depression.[2] The principal pathological feature of PD is degradation of the dopaminergic nigrostriatal neurons.[3] The neuronal cell bodies are located in the substantia nigra and project to the basal ganglia where the dopamine is stored and released. Another aspect of the pathology of PD is the formation of protein inclusion structures known as Lewy bodies. Their function in the brain is currently unknown.

---

[1] Isin, E. M. (2000) Potential prodrugs of neuronal nitric oxide synthase and monoamine oxidase inhibitor 7-nitroindazole and structurally related compounds. M. S. Thesis, VPI & SU, Blacksburg, VA, 2000.

[2] Fahn, S., Przedborski, S. (2000) Parkinsonism. In *Merritt's Neurology* (Rowland, L. P., ed.) pp. 679-693, Lippincott Williams & Wilkins, New York.

[3] Hornykiewicz, O., Kish, S. J. (1984) *Parkinson's Disease*. 19-34

### 1.2 MPTP and PD

MPTP (**2**), a byproduct of an illicit drug synthetic effort, is a neurotoxin. The street drug was known as China White and was designed to be a heroin-like substance. The targeted compound, **3**, is an isomer of meperidine (**4**). This meperidine analog, however, was contaminated with MPTP because the individual trying to synthesize **3** took shortcuts during the synthesis. It was discovered that the reaction conditions had a dramatic influence on the extent to which the MPTP byproduct was produced.[4] More vigorous reaction conditions caused the dehydration of 1-methyl-4-phenyl-4-piperidinol (**6**, Scheme 1) to give MPTP. MPTP also is formed by acid treatment of **3**. When drug abusers in California injected this mixture, they developed parkinsonian like symptoms.[5] The symptoms of and response to treatment for this condition were similar to those characteristic of idiopathic PD.

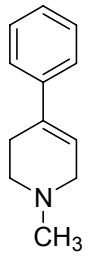


**2**

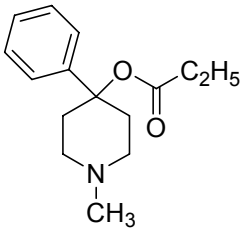


**3**

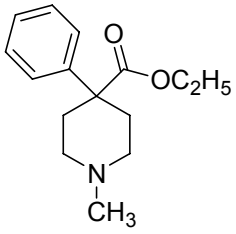


**4**

[4] Ziering, A., Berger, L., Heineman, S. D., Lee, J. (1947) Piperidine derivatives: Part III. 4-Aryl piperidines. *J. Org. Chem.* **12**, 894-903.

[5] Langston, J. W., Ballard, P., Tetrud, J. W., Irwin, I. (1983) Chronic parkinsonism in humans due to a product of mepiridine-analog synthesis. *Science*. **219**, 979-980.

**Scheme 1. Formation of MPTP**

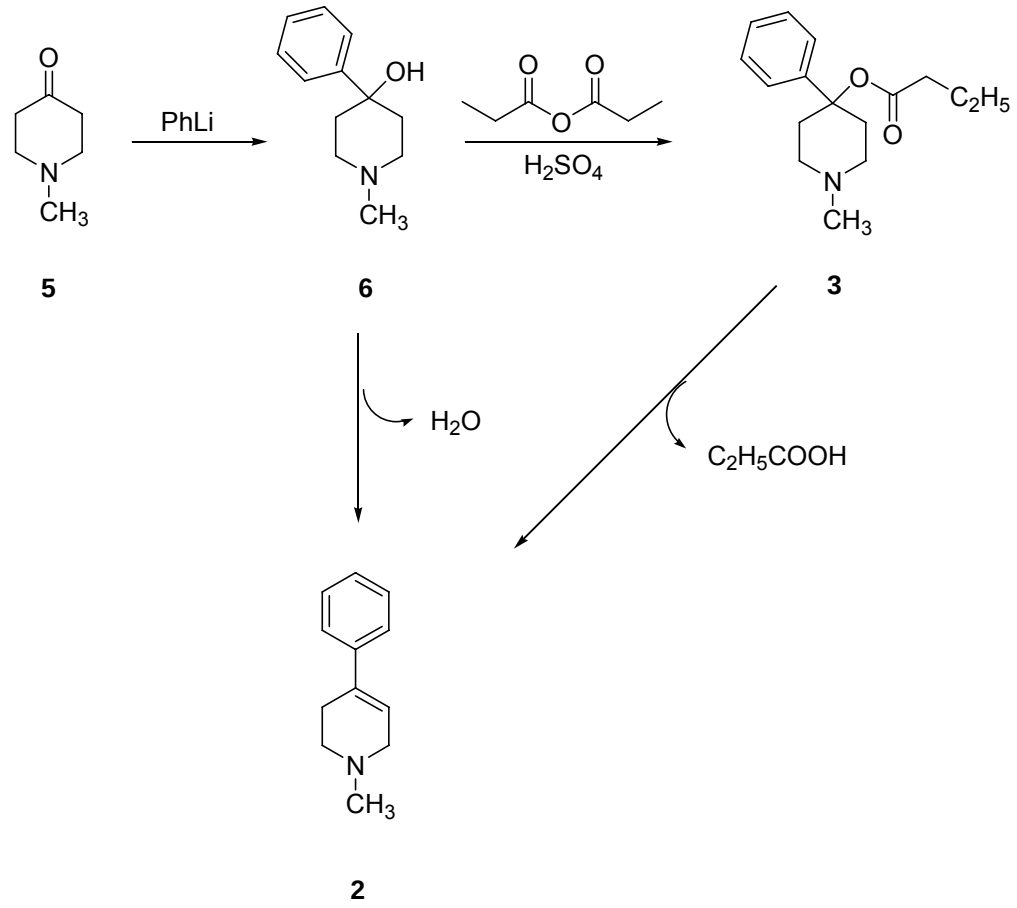


An inspection of the structure of MPTP did not suggest any obvious mechanism by which it would exert such toxic effects. This led to the speculation that the parent compound may undergo metabolic bioactivation to generate toxic species that mediate this toxicity.[6] MPTP was shown to be a substrate for the flavoenzyme monoamine oxidase-B (MAO-B) that catalyzes its conversion into the 1-methyl-4-phenyl-2,3-dihydropyridinium metabolite $MPDP^+$ (**7**). This intermediate is then further oxidized to generate the ultimate neurotoxin, the 1-methyl-4-phenylpyridinium species $MPP^+$ (**8**).[7]

---

[6] Sayre, L.M., Arora, P.K., Iacofano, L.A., Harik, S.I. (1986) Comparative toxicity of MPTP, MPP+ and 3,3-dimethyl-MPDP+ to dopaminergic neurons of the rat substantia nigra. *Eur J Pharmacol*. **124**, 171-174.

[7] Salach, J. I., Singer, T. P., Castagnoli, N., Jr. Trevor, A. (1984) Oxidation of the neurotoxic amine 1-methyl-1,2,3,6 tetrahydropyridine (MPTP) by monoamine oxidases A and B and suicide inactivation of enzymes by MPTP. *Biochem Biophys. Res. Commun.* **125**, 831-835.

The conversion of MPTP into the $MPP^+$ (Scheme 2) occurs in the glial cells.[8] $MPP^+$ is then taken up into the dopaminergic nerve terminals by the dopamine transporter.[9] This neurotoxin ultimately builds up in the inner mitochondrial membrane where it inhibits Complex I of the respiratory chain leading to energy deficits and eventually cell death.[10] MPTP has provided the research community with a powerful tool to study of PD. Since its discovery in 1983, there have been 6,661 publications involving MPTP according to Scifinder (2005).

**Scheme 2. MAO-B catalyzed oxidation of MPTP**

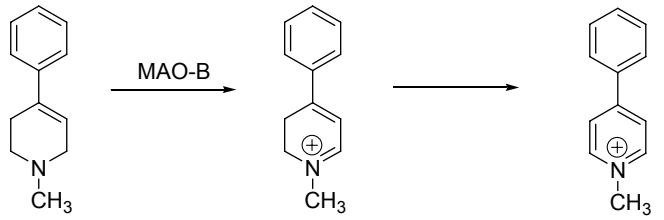


**2** **7** **8**

### 1.3 PD and Oxidative Stress

Despite extensive studies over the past 100 years, the etiology of PD remains unclear. One proposal is based on the concept of oxidative stress.[11] This hypothesis proposes that reactive oxygen species generated in the substantia nigra react with macromolecules (DNA, proteins and lipids) to bring about cellular dysfunction and eventually cell death. Nitric oxide (NO) derived species, such as peroxynitrite and nitrogen dioxide (see below) are thought to mediate some of these toxic outcomes. The enzyme that catalyzes the formation of NO, nitric oxide synthase (NOS), catalyzes the conversion of *L*-arginine (**9**) into *L*-citrulline (**11**) and NO (**12**). It has been argued that inhibition of NOS and the production of NO could prevent oxidative stress. These

[8] Di Monte, D.A., Wu, E.Y., Irwin, I., DeLanney, L.E., Langston, J.W. Biotransformation of 1-methyl-4-phenyl-1,2,3,6-tetrahydropyridine in primary cultures of mouse astrocytes. (1991) *J Pharmacol Exp Ther*. **258**, 594-600.

[9] Javitch, J.A., D'Amato, R.J., Strittmatter, S.M., Snyder, S.H. Parkinsonism-inducing neurotoxin, N-methyl-4-phenyl-1,2,3,6-tetrahydropyridine: Uptake of the metabolite N-methyl-4-phenylpyridine by dopamine neurons explains selective toxicity. (1985) *Proc Natl Acd Sci USA*. **82**, 2173-2177.

[10] Cleeter, M. W. J., Cooper, J. M., and Schapira, A. H. V. (1992) Irreversible inhibition of mitochondrial complex I by 1-methyl-4-phenylpyridinium: Evidence for free radical involvement. *J. Neurochem.* **58**, 786-789.

[11] Przedborski, S., Jackson-Lewis, V. (2000) ROS and Parkinson's disease: a view to a kill. *In: Free Radicals in Brain Pathophysiology*. pp. 273-290.

considerations have led to an interest in inhibitors of NOS and, in particular, the neuronal form of NOS, i.e. nNOS.

**Scheme 3. Conversion of *L*-Arginine into *L*-Citrulline by NOS**

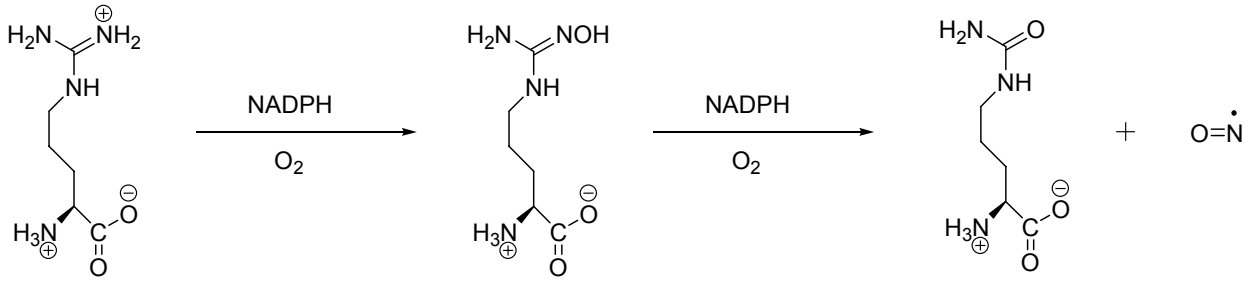


**9** **10** **11** **12**

NO (**12**), the endothelium derived relaxing factor (EDRF),[12] was first identified in 1987 in vascular endothelial cells. In addition to being a potent vasodilator, it has neurotransmitter properties as well.[13] The 15-electron structure of NO (Fig. 1) has an unpaired electron in a 2p-$\pi$ antibonding orbital. The lone electron in the 2p-$\pi$ bonding orbital gives this diatomic molecule a bond order of 2.5. Important resonance forms (**12a** $\leftrightarrow$ **12b**) for NO can be written. NO is a gaseous molecule that distributes into intra- and extra-cellular spaces with a half-life of only a few seconds.[14]

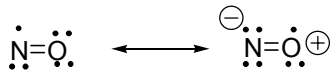

**12a** **12b**

[12] Ifnarro, L. J., Byrns, R, E., Buga, G.M., Wooks, K. S. (1987) Endothelium-derived relaxing factor from pulmonary artery and vein possesses pharmacological and chemical properties that are identical to those for nitric oxide radical. *Circ. Res.* **61**, 866-879.
[13] Schwartz, J. H. (2000) Neurotransmitters. *In: Principles of Neural Science 4th Ed.* pp. 280-297.
[14] Bredt, D. S., Synder, S. H. (1994) Nitric oxide: a physiologic messenger molecule. *Ann Rev Biochem*. **63**, 175-95.

**Figure 1. Molecular orbital description of NO**

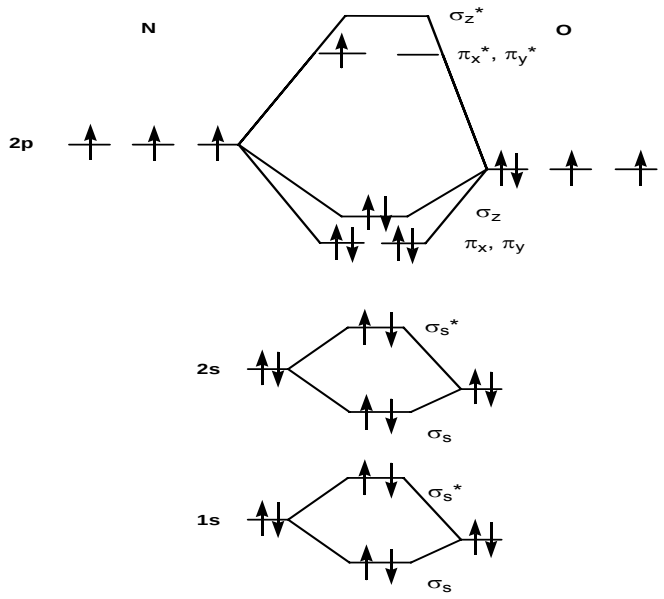


NO exerts its effects in the brain in multiple ways. Some of the cellular actions of NO include guanylate cyclase activation and production of the intracellular second messenger c-GMP.[15] This second messenger regulates ion currents and neurotransmitter release, which ultimately contributes to the long-term potentiation of nerve signals and memory. NO has been shown to effect synaptic plasticity and therefore it is particularly important in long-term memory.[15] NO also activates NMDA receptors, mediating glutamate release.[17] An excess of glutamate or other excitotoxins may lead to cell induced necrosis due to elevated levels of $Ca^{2+}$ and $Na^{+}$. Consequently, excess production of NO can ultimately lead to neurodegenerative diseases such as PD. Exposure to excessive amounts of NO can lead to covalent modifications of –SH groups and damage to iron-sulfur proteins in mitochondria. Mitochondrial damage is not mediated directly by NO but rather from NO-derived oxidation products.[16] For example, NO-derived nitrogen oxides nitrosylate thiols such as cysteine or cysteinyl residues.[17]

---

[15] Ferhan, G. S., Eser, Y., Sozmen, B. E., Gulriz M. (2004) Link between monamine oxidase and nitric oxide. *NeuroToxicology*. **25**. 91-99.

[16] Blanchard, B., Dendane, M., Gallard, J. F., Houee-Levin, C., Karim, A., Payen, D. Launay, J-M., Ducrocq, C. (1997) Oxidation, nitrosation, and nitration of serotonin by nitric oxide-derived nitrogen oxides: Biological implications in the rat vascular system. *Nitric Oxide Biol. Chem*. **1**, 442-452.

[17] Goldstein, S., Czapski, G. (1996). Mechanisms of the nitrosation of thiols and amines by oxygenated solutions: The nature of the nitrosating intermediates. *J. Am. Chem. Soc.* **118**, 3419-3425.

Some of these toxic nitrogen species include dinitrogen trioxide (**13**)**,** peroxynitrite (**14**), and peroxynitrous acid (**15**).[17] Compound **14** is reported to oxidize glutathione, ascorbate, and tocopherol and to nitrate tyrosinnyl residues in proteins.[18] The routes leading to the formation of these NO-derived species are shown below.

**Scheme 4. Nitrosylation of thiols**

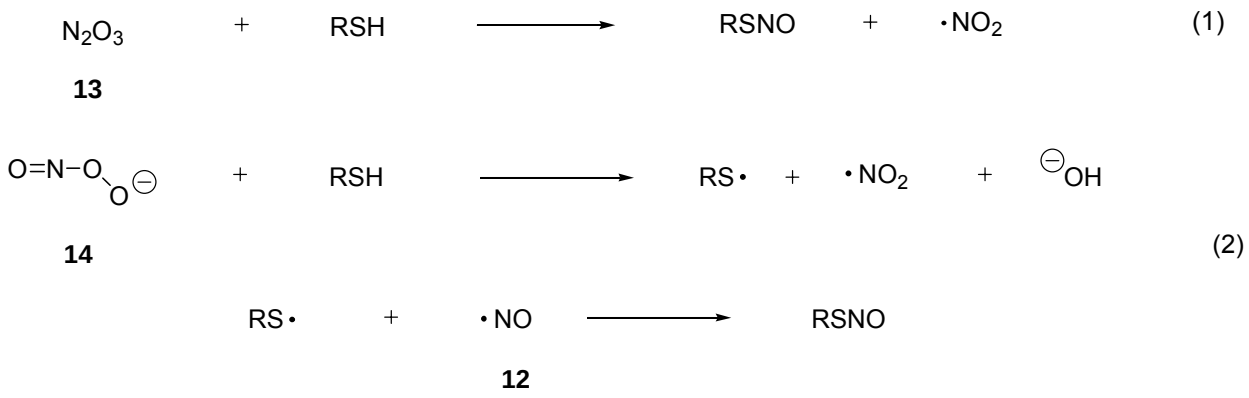


**Scheme 5. Formation of dinitrogen trioxide (13)**

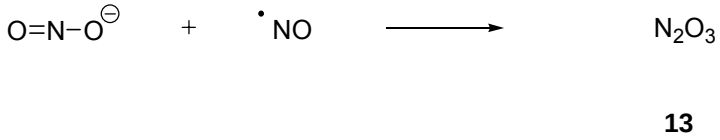


**Scheme 6. Formation of peroxynitrite (14)**

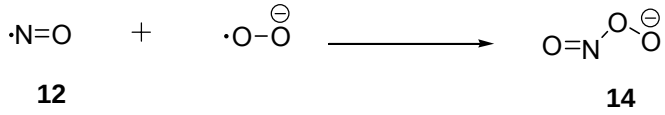


**Scheme 7. Equilibrium reaction of 14 with protonated form of peroxynitrous acid 15**

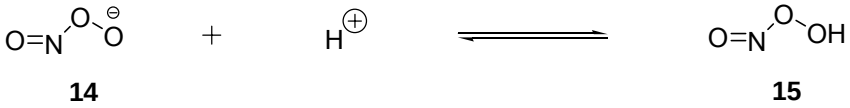


[18] Pryor, W. A., and Squadrito, G. L. (1995). The chemistry of peroxynitrite: A product from the reaction of nitric oxide with superoxide. *Am. J. Physiol.* **268**, L699-L722.

### 1.4 nNOS Inhibition by Indazoles

In 1993, 7-nitroindazole (7-NI, **1**) was found to be a selective inhibitor of nNOS *in vivo*.[19] The isomeric 5- and 6-nitroindazoles [5-NI (**16a**) and 6-NI (**17a**)] were found to inhibit nNOS *in vivo* in the same study. While the $IC_{50}$'s of 5- and 6-NI were 47.3 μM and 31.6 μM, respectively, the $IC_{50}$ value of 7-NI was determined to be 0.900 μM. This means that 5- and 6-NI are 52.5 and 35.1 times less potent nNOS inhibitors than 7-NI.

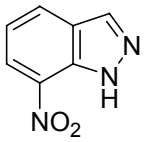

**1**

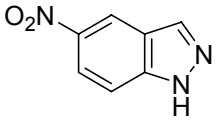

**16a**

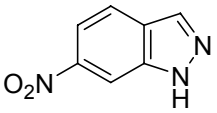

**17a**

### 1.5 Monoamine Oxidase (MAO)

MAO is a flavin (**18**) containing enzyme that is found throughout the human body and is localized in the outer mitochondrial membrane.[20] Two forms of the enzyme, MAO-A and MAO-B, are known.[21] These are the principal enzymes involved in the metabolism of the neurotransmitters dopamine (**19**), norepinephrine (**20**), epinephrine (**21**), and serotonin (**22)**.[22]

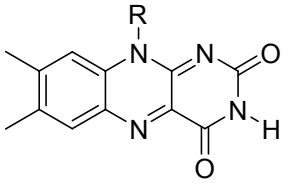

**18**

---

[19] Babbedge, R. C., Bland-Ward, P. A., Hart, S. L., Moore, P. K. (1993) Inhibition of rat cerebellar nitric oxide synthase by 7-nitroindazole and related substituted indazoles. *Br. J. Pharmacol.* **110**, 225-228.

[20] Inoue, H., Castagnoli, K., Van der Schyf, C., Mabic, S., Igarashi, K., Castagnoli, N., Jr. (1999) Species-dependent differences in monoamine oxidase A and B-catalyzed oxidation of various C4 substituted 1-methyl-4-phenyl-1,2,3,6-tetrahydropyridinyl derivatives. *The Journal of Pharmacology and Experimental Therapeutics*. **291**, 856-864.

[21] Johnston, J. P. (1968) Some puzzling pharmacological effects of monoamine oxidase inhibitors. *Biochem Pharmacol.* **17**, 1285-1297.

[22] Waldmeier, P. C. (1987) Amine oxidases and their endogenous substrates. *J. Neural Transmission Suppl.* **23**, 55-72.

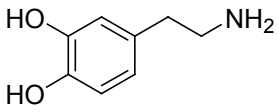

**19**

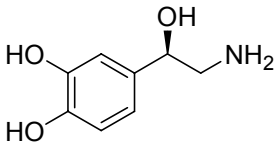

**20**

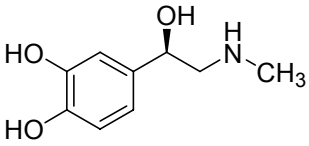

**21**

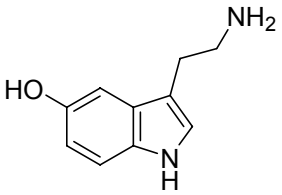

**22**

The highest levels of MAO-A in humans are found in the liver, lung, and intestines while the highest levels of MAO-B are found in the brain and liver.[23] Both forms of MAO have highly selective substrates while some substrates overlap in enzyme activity and can fit into both active sites. Since the neurodegenerating properties of MPTP are dependent on its selective MAO-B substrate properties,[7] inhibition of this form of the enzyme results in neuroprotection against the resulting toxicity.

### 1.6 MPTP and 7-NI

Further studies on 7-NI showed it to protect against MPTP-induced neurotoxicity in animals.[24,25] Originally, it was thought that these neuroprotective effects were mediated exclusively by the nNOS inhibiting properties of this compound. In a separate study, a comparison was made between 7-NI injected and control mice, both of which had been treated with MPTP. The results showed that the striatal $MPP^+$ levels were unaffected[26] and led the authors to conclude that the neuroprotective effects of 7-NI were primarily

---

[23] Squires, R. F. (1972) Multiple forms of monoamine oxidase in intact mitochondria as characterized by selective inhibitors and thermal stability: a comparison of eight mammalian species. *Monoamine Oxidases-NewVistas*. E. Costa; M. Sandler. New York, Raven Press: 355-370.

[24] Hantraye, P., Brouillet, E., Ferrante, R., Palfi, S., Dolan, R., Matthews, R. T., Beal, M. F. (1996) Inhibition of neuronal nitric oxide synthase prevents MPTP-induced parkinsonism in baboons. *Nature Med.* **64**, 936-939.

[25] Schulz, J. B., Matthew, R. T., Muqit, M. M., Browne, S. E., Beal, M. F. (1995) Inhibition of neuronal nitric oxide synthase by 7-nitroindazole protects against MPTP-induced neurotoxicity in mice. *J. Neurochem.* **64**, 936-939.

[26] Przedborski, S., Jackson-Lewis, V., Yokoyama, R., Shibata, T., Dawson, V. L., Dawson, T. M. (1996) Role of neuronal nitric oxide in 1-methyl-4-phenyl-1,2,3,6-tetrahydropyridine (MPTP)-induced dopaminergic neurotoxicity. *Proc. Natl. Acad. Sci. USA* **93**, 4565-4571.

due to nNOS inhibition. Of note is the planarity of 7-NI,[27] since it is known that a wide variety of planar, heterocyclic compounds are inhibitors of MAO-B.[28,29] This prompted direct studies on the MAO-B inhibition properties of 7-NI[30] and established that 7-NI is a competitive inhibitor of this enzyme. The $K_i$ value of 7-NI was found to be 40 μM in semi-purified beef liver MAO-B and 4 μM in mouse brain mitochondrial preparations.[31] Furthermore, 7-NI was found to protect mice against the MPTP induced depletion of neostriatal dopamine.[32] It was observed that the striatal levels of $MPP^+$ were decreased in the 7-NI treated animals. These results suggested that the neuroprotective properties of 7-NI were at least in part due to MAO-B inhibition.

The poor solubility of 7-NI limited the type of studies that could be performed with this compound. Therefore, novel approaches to provide a 7-NI prodrug (see below) with better solubility properties were undertaken.[1]

The MAO-B inhibition properties of 5- and 6-NI also have been examined. The $K_i$ values for 5- and 6-NI (**16a** and **17a**) were established to be 5 μM and 12 μM, respectively.[1] They are as potent MAO-B inhibitors as 7-NI and therefore merited examination in more detail as prodrugs. Furthermore, it was found that the structurally related 5-nitrobenzimidazole (**23**) had a $K_i$ value of 42 μM for baboon liver mitochondrial MAO-B and also needed to be examined in more detail as a potential prodrug.[33]

---

[27] Odoms, F., Norberg, B., Isin, E. M., Castagnoli, N., Van der Schyf, C. J., Wouter, J. (2000) 7-Nitroindazole. *Acta Cryst. C* **56**, 474-475.

[28] Kneubuehler, S., Thull, U., Altomare, C., Carta, V., Gaillard, P., Carrupt, P. A., Carotti, A., Testa, B. (1995) Inhibition of monoamine oxidase-B by 5H-Indeno[1,2-c]pyridazines. Biological activities, quantitative structure-activity relationships (QSARs) and 3D-QSARs. *J. Med. Chem.* **38**, 3974-3883.

[29] Lebreton, L., Curet, O., Gueddari, S., Mazouz, F., Bernard, S., Burstein, c., Milcent, R. (1995) Selective and potent monamine oxidase type B inhibitors: 2-substituted 5-aryltetrazole derivatives. *J. Med. Chem.* **38**, 4786-4792.

[30] Castagnoli, K., Palmer, S., Anderson, A., Bueters, T., Castagnoli, N., Jr. (1998) The neuronal nitric oxide synthase inhibitor 7-nitroindazole also inhibits the monamine oxidase-B catalyzed oxidation of 1-methyl-4-phenyl-1,2,3,6-tetrahydropyridine. *Chem. Res. Toxicol.* **11**, 716-717.

[31] Castagnoli, K., Palmer, S., Anderson, A., Bueters, T., Castagnoli, N., Jr. (1997) The neuronal nitric oxide synthase inhibitor 7-nitroindazole also inhibits the monoamine oxidase-B-catalyzed oxidation of 1-methyl-4-phenyl-1,2,3,6-tetrahydropyridine. *Chem. Res. Toxicol.* **10**, 364-368.

[32] Di Monte, D. A., Royland, J. E., Anderson, A., Castagnoli, K., Castagnoli, N., Jr., Langston, J. W. (1997) Inhibition of monoamine oxidase contributes to the protective effect of 7-nitroindazole against MPTP neurotoxicity. *J. Neurochem.* **69**, 1771-1773.

[33] Annette van Utteren

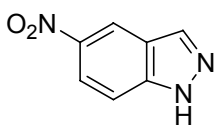

**16a**

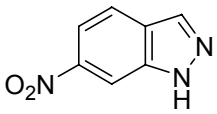

**17a**

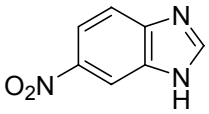

**23**

## 1.7 Prodrugs

The prodrug concept was first introduced in 1958 by Adrien Albert.[34] According to Testa, prodrugs are compounds that undergo biotransformation prior to eliciting their pharmacological effects.[35] The main advantage of a prodrug is the possibility to control the delivery of the active drug. There are several important criteria for this delivery system to be successful. These include improving the transport of the active drug to the desired receptor before the drug is cleared, maintaining an appropriate drug plasma concentration, increasing shelf life, improving the taste, increasing solubility, improving the properties of injectables, and improving the process of making tablets.[36]

Prodrugs are classified by two criteria.[34] One of these criteria is the chemical class to which the compound belongs. For instance, there are carrier-linked prodrugs, bioprecusors, macromolecular prodrugs, and drug-antibody conjugates. Carrier-linked prodrugs are those in which the active drug is linked to a carrier and activation occurs by hydrolysis, oxidation, or reduction.[37] Carrier-linked prodrugs are further classified into three categories. They include bipartate, tripartate and mutual prodrugs. Bioprecursors prodrugs do not contain the promoiety (carrier). However, they are still activated by hydrolysis, oxidation, or reduction.[38] Macromolecular prodrugs are those in which the carrier of the active drug is a macromolecule. This approach has been used in the design of produgs of anti-cancer agents in which the active compound was linked to a

---

[34] Albert, A. (1958) Chemical Aspects of selective toxicity. *Nature*, **182** 421-422.
[35] Ettmayer, P., Amidon, G. L., Clement, B., Testa, B. (2004) Lessons learned from marketed and investigational prodrugs. *J. Med. Chem.* **47**, 2393-2404.
[36] Stella, V. J., Charman, W. N., Naringrekar, V. H. (1985) Prodrugs. Do they have advantages in clinical practice? *Drugs* **29**, 455-473.
[37] Testa, B. (2004) Prodrug research: futile or fertile. *Biochemical Pharmacology*. **68**, 2097-2106.
[38] Wermuth, C. G. *Designing prodrugs and bioprecusors: In: Drug Design: Fact or Fantasy?* London; Academic Press. **1984**. pp. 47-72

polyethyleneglycol carrier.[39] The final classification for chemical classes is drug-antibody conjugates in which the carrier is an antibody that attempts to utilize a cytotoxic species and target tumor cell markers.[40] The carrier-linked prodrugs and bioprecursors are the largest groups of prodrugs currently being used.[38]

A variety of approaches to the design of prodrugs can be cited. One such example is the use of esters as prodrugs of compounds that contain either a carboxyl or a hydroxyl group. These types of prodrugs protect the functionalities of the active compound from metabolic clearance.[41] The active compound is released upon hydrolysis of the ester. Other examples of prodrugs include inactive compounds which are bioactivated via reductive or oxidation pathways.[42]

The application of the prodrug concept which we are interested in pursuing involves the tetrahydropyridyl group as the carrier moiety. This group has been used in the past in the construction of analogs of the well-studied MAO-B selective substrate MPTP (**2**).[43] The tetrahydropyridyl group has been used to develop the carbamate prodrug **24**, a compound with MAO-B inhibitor properties that are mediated by the active inhibitor (*R*)-nordeprenyl (**25**).[44] The bioactivation pathway is present in **Scheme 8**. Initially, **24** is oxidized to the dihydropyridinium species (**26**). This is followed by hydrolysis to give the aminoenone (**27**) and the carbamic acid (**28**). Subsequent decarboxylation results in the formation of (*R*)-nordeprenyl (**25**). An attractive feature of this approach is the possibility of targeting the central nervous system that has high levels of MAO-B activity.

---

[39] Duncan, R. (1992) Drug-polymer conjugates: potential for improved chemotherapy. *Anti-Canc Drugs*. *120*, 175-210.

[40] Dubowchik, G. M., Walker, M. A. (1999) Receptor-mediated and enzyme-dependent targeting of cytotoxic anticancer drugs. *Pharmacol. Therapy*. *83*, 67-123.

[41] Bundgaard, H. Design of prodrugs: Bioreversible derivatives for various functional groups and chemical entities. *Design of prodrugs*; Elsevier Science Publishers B. V. (Biomedical Division ): Amsterdam, 1985; pp 1-92.

[42] Nicoll-Griffith, D. A., Falgueyret, J. P., Silva, J. M., Morin, P. E., Trimble, L, Chan, C. C., Clas, S., Leger, S., Wang, Z., Yergey, J. A., Riendeau, D. (1999) Oxidative bioactivation of lactol prodrug of a lactone cycloxygenase-2 inhibitor. *Drug. Metab. Dispos.* **27**, 403-409.

[43] Zhao, Z.; Dalvie, D.; Naiman, N.; Castagnoli, K. P.; Castagnoli Jr., N. (1992) Design, synthesis, and biological evaluation of novel 4-substituted 1-methyl-1,2,3,6-tetrahydropyridine analogs of MPTP. *J. Med. Chem.* **35**, 4473-4478.

[44] Flaherty, P., Castagnoli, K., Wang, T. W., Castagnoli, N., Jr. (1996) Synthesis and selective monamine oxidase B-inhibiting properties of 1-methyl-1,2,3,6-tetrahydropyrid-4-yl carbamate derivatives: Potential prodrugs of (*R*)- and (*S*)-nordeprenyl. *J. Med. Chem.* **39**, 4756-4761.

**Scheme 8: MAO-B bioactivation of nordeprenyl prodrug**

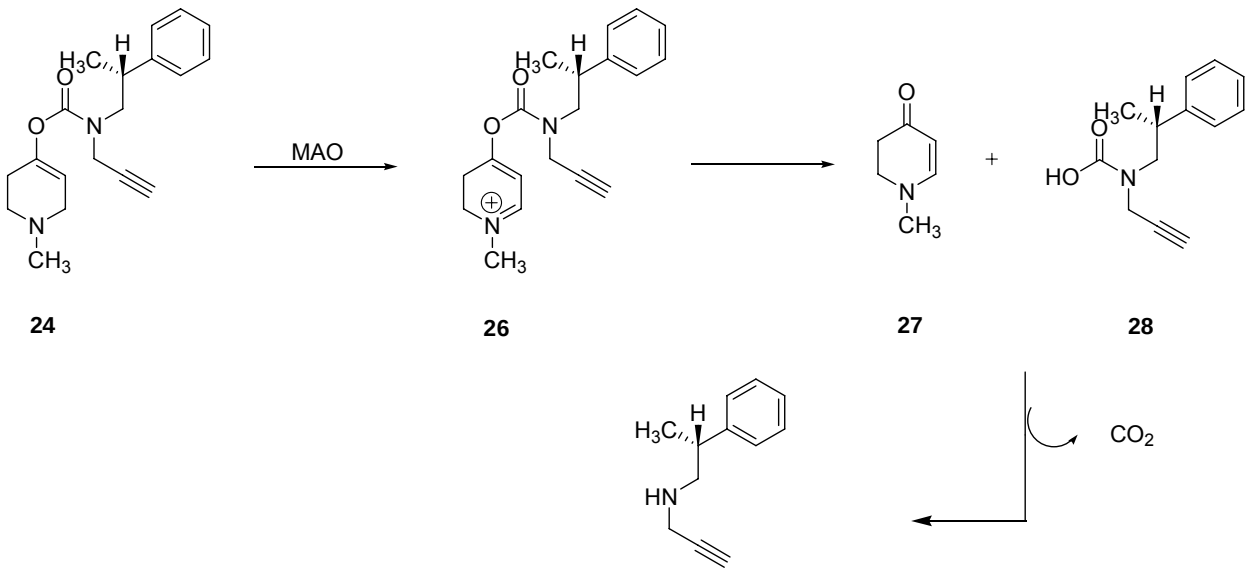


**24** **26** **27** **28** **25**

## 1.8 MAO properties of prodrugs previously synthesized

Isin studied the MAO substrate properties of the prodrugs **29**, **31**, and **33**.[1] Isin also has attempted the synthesis of the regioisomers **30**, **32**, and **34** but was not successful.

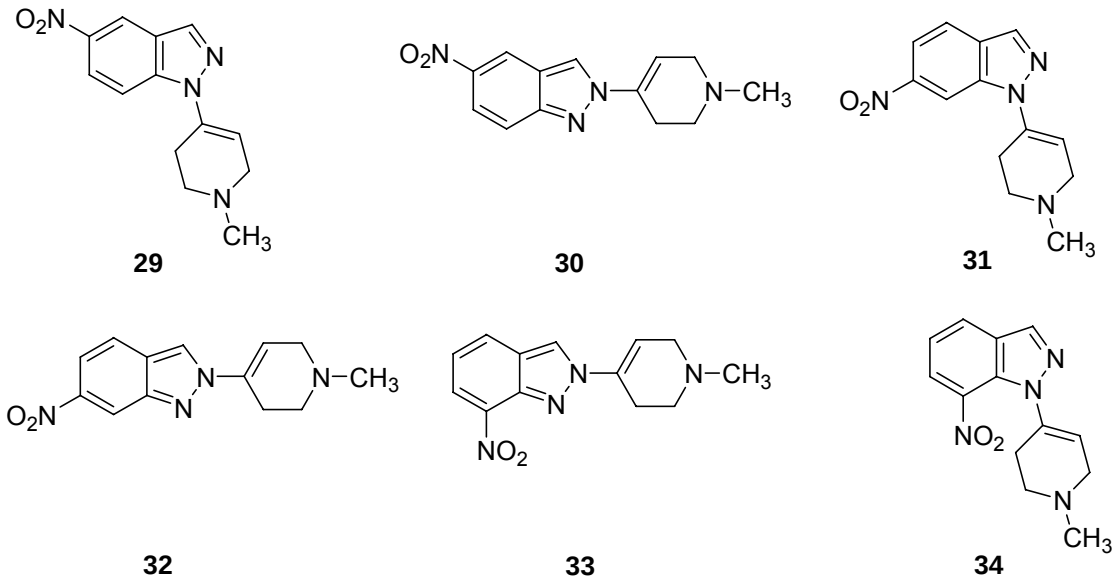

**29** **30** **31** **32** **33** **34**

Isin determined that **33** was not a substrate for either MAO-A or MAO-B. These results were obtained with HPLC-DA assays of incubation mixtures and monitoring metabolite formation.[1] While this was the outcome for the 7-NI prodrug **33**, prodrugs **29** and **31** were both found to be substrates for MAO-B. However, only **31** showed MAO-A activity in the 5- and 6-NI indazolyl prodrug series. The $K_m$ value of **29** with MAO-B was estimated to be 50 μM while the $K_m$ of **31** with MAO-B was not determined.

As shown in **Scheme 9A**, metabolites generated from the reaction of MAO-B with both **29** and **31** were identified as the corresponding pyridinium species (**40** and **41**). The parent indazoles **16** and **17** also were detected possibly as the result of hydrolysis. This led to the question as to why the structurally related analog 1-methyl-4-benzimidazol-1-yl-1,2,3,6-tetrahydropyridine (**35**) primarily undergoes hydrolysis[45] to **36** (**Scheme 9B**) rather than further oxidation as observed with the indazolyl prodrugs.

**Scheme 9A: Reactions leading to a pyridiniums species**

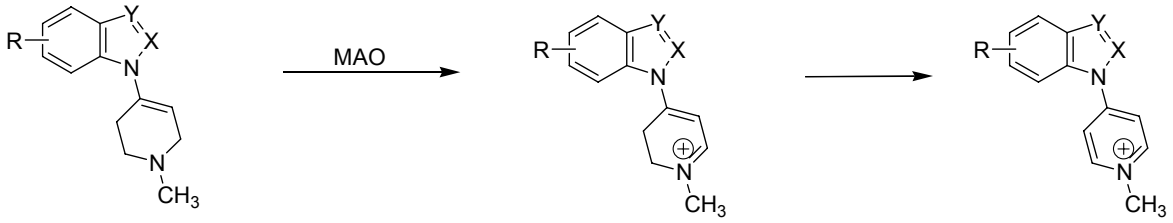


**29** : R = 5-$NO_2$ , Y = CH, X = N
**31** : R = 6-$NO_2$ , Y = CH, X = N
**35** : R = H , Y = N, X = CH

**37** : R = 5-$NO_2$ , Y = CH, X = N
**38** : R = 6-$NO_2$ , Y = CH, X = N
**39** : R = H , Y = N, X = CH

**40** : R = 5-$NO_2$ , Y = CH, X = N
**41** : R = 6-$NO_2$ , Y = CH, X = N
**42** : R = H , Y = N, X = CH

[45] Nimkar, S. K., Mabic, S., Anderson, A. H., Palmer, S. L., Graham, T. H., de Jonge, M., Hazelwood, L., Hislop, S. L., Castagnoli, N., Jr. (1999) Studies on the monoamine oxidase-B-catalyzed biotransformation of 4-azaaryl-1-methyl-1,2,3,6-tetrahydropyridine derivatives. *J. Med. Chem.* **42**, 1828-1835.

**Scheme 9B: Reactions leading to a hydrolysis product**

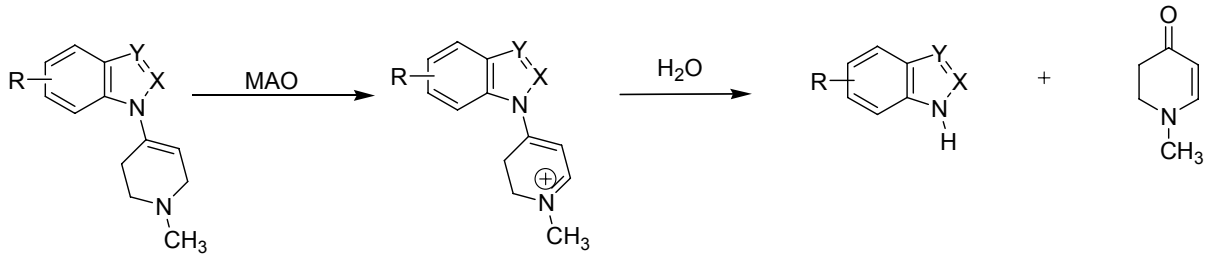


**29** : R = 5-$NO_2$ , Y = CH, X = N
**31** : R = 6-$NO_2$ , Y = CH, X = N
**35** : R = H , Y = N, X = CH

**37** : R = 5-$NO_2$ , Y = CH, X = N
**38** : R = 6-$NO_2$ , Y = CH, X = N
**39** : R = H , Y = N, X = CH

**16a** : R = 5-$NO_2$ , Y = CH, X = N
**17a** : R = 6-$NO_2$ , Y = CH, X = N
**36** : R = H , Y = N, X = CH

**27**

A possible rationale for these differences in behavior is presented in **Scheme 10**. During the hydrolytic cleavage of the 1*H*-prodrug metabolites (**37** and **38**), the product formed would be the less stable 2*H*-tautomers (**16b** and **17b** respectively) and not the 1*H*-tautomer. The 2*H*-tautomer lacks the benzenoid structure and would thus be less stable than either the benzimidazole or the 1*H*-tautomer. This would make oxidation to the pyridinium species more favored for these 1*H*-prodrugs.

**Scheme 10: Hydrolytic cleavage of 1*H*-prodrug metabolites**

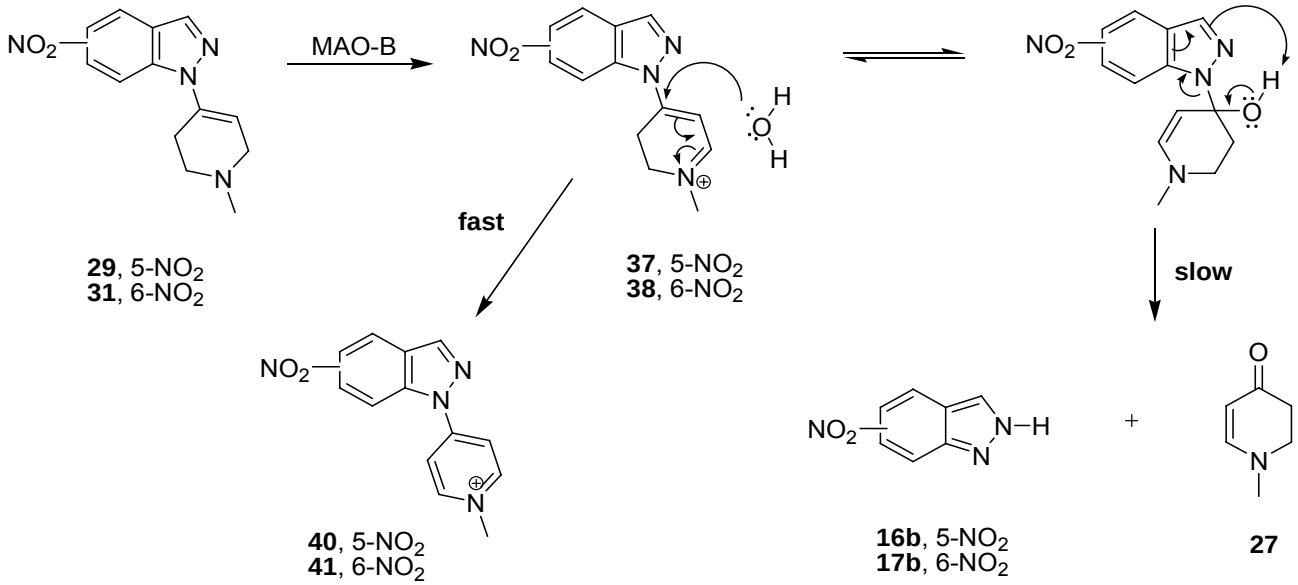


**29**, 5-$NO_2$
**31**, 6-$NO_2$

**37**, 5-$NO_2$
**38**, 6-$NO_2$

**40**, 5-$NO_2$
**41**, 6-$NO_2$

**16b**, 5-$NO_2$
**17b**, 6-$NO_2$

**27**

The MAO substrate properties of 1-methyl-4-(5-nitrobenzimidazol-1-yl)-1,2,3,6-tetrahydropyridine (**43**) also have been examined.[46] This compound proved to be a substrate for MAO-B with the release of 5-nitrobenzimidazole (**23**) as a major metabolite following bioactivation. The pathway to account for the formation of this metabolite is the same as that proposed for **35** above (**Scheme 9**) except that R = 5-$NO_2$ for this case. The other regioisomer (**64**) of this series was never synthesized.

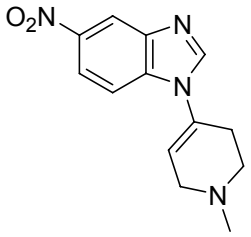

**43**

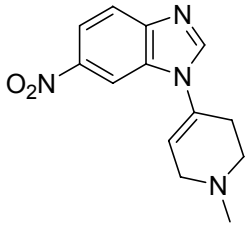

**64**

[46] van Utteran, Annette. (2001) MAO activity of a series of benzimidazolyl prodrugs. Laboratory Progress Report, Peters Center, Chemistry Department, Va Tech, Blacksburg, VA Neal Castagnoli Jr. Director

## 2.0 Chemistry: Review of earlier synthetic studies on indazoles

In the past, nucleophilic aromatic substitution reactions have been applied to the synthesis of various indazolyl derivatives related to the prodrug theme. One example of this synthetic approach is given for the synthesis of the 1*H*- and 2*H*-pyridinyl analogs **46** and **47**, respectively. In this reaction indazole (**44**) is treated with 4-fluoropyridine (**45**) to give the indicated products.[47] Unfortunately, as discussed below, this reaction suffers from some serious drawbacks. Following this step, methylation of the nitrogen atom on the pyridine ring gives the corresponding pyridinium intermediates **48** and **49** which can be reduced to the desired candidate prodrugs with $NaBH_4$.

**Scheme 11:** Formation of **46** and **47**

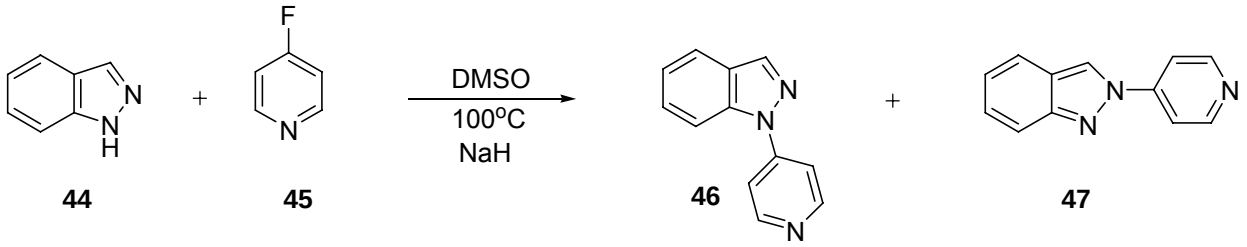


**44** **45** **46** **47**

[47] Emre M. Isin, Milly de Jonge, Neal Castagnoli Jr. (2001) Studies on Synthetic Approaches to 1H- and 2H-Indazolyl Derivatives. *Journal of Organic Chemistry.* **66**, *12*, 4220-4226.

**Scheme 11 (cont.):** Formation of **46** and **47**

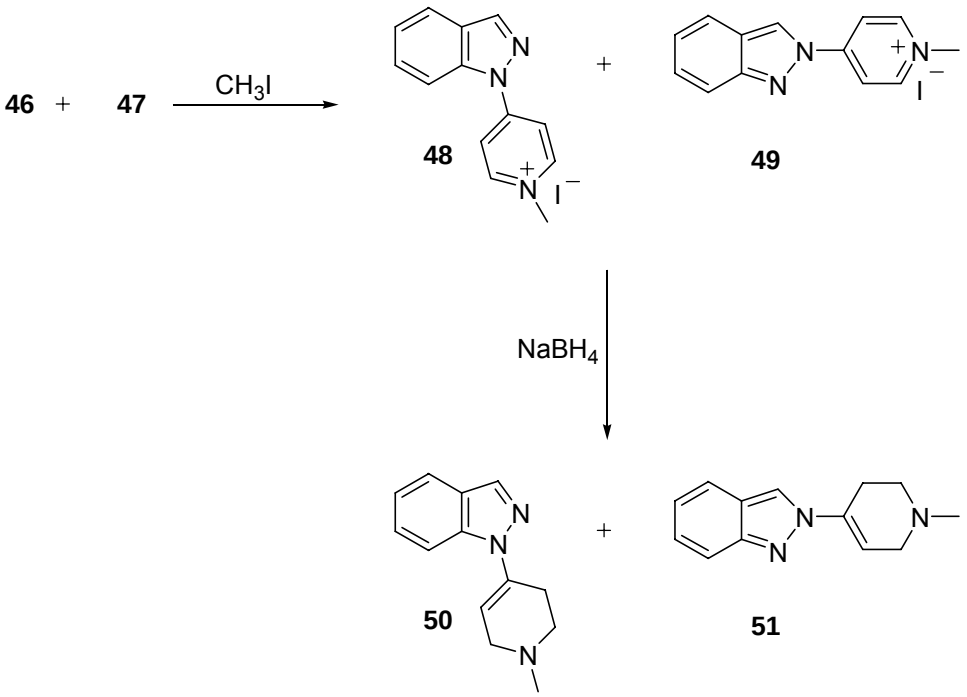


While this is a useful approach to synthesizing the desired prodrug analogs, one must use HF (a very hazardous gaseous material) in the process to synthesize **45**. Furthermore, the yields were only modest. Consequently other reactions were explored. Two of these involved ring closing routes. **Scheme 12** illustrates a pathway involving condensation of 4-pyridinylhydrazine (**52**) with *o*-fluorobenzaldehyde (**53**) followed by treatment of the resulting adduct **50** with NaH in DMF. However, the cyclization step (**54** → **46**) failed. The reaction shown in **Scheme 13** was also attempted. Although the alkylation of 4-aminopyridine (**55**) with *o*-nitrobenzyl bromide (**56**) proceeded efficiently to give **57** in 89% yield, the conversion of **57** into **47** was unsuccessful.[47]

**Scheme 12: Formation of 46**

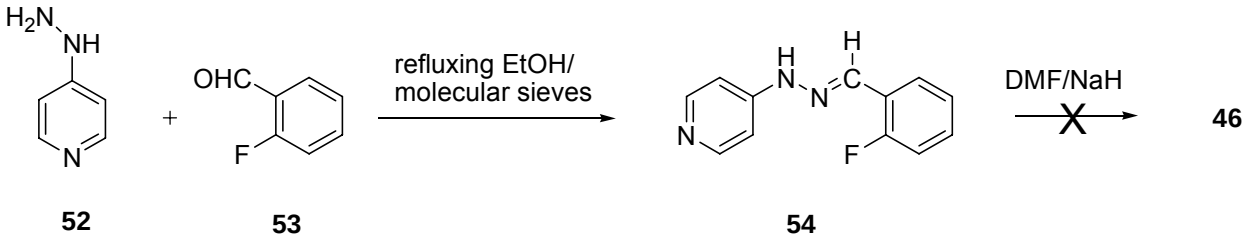


**52** **53** **54**

**Scheme 13: Formation of 47**

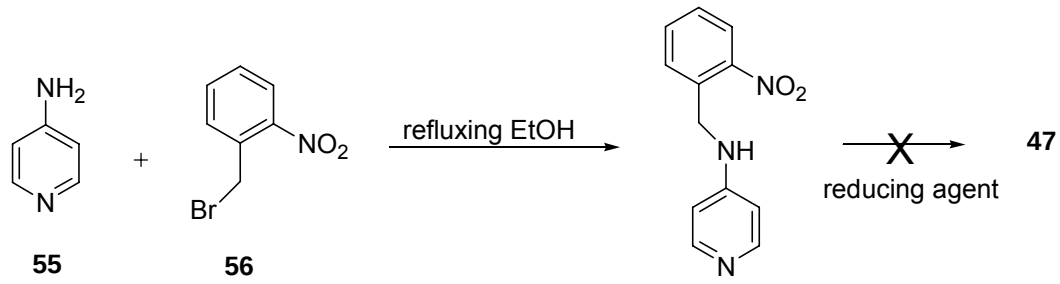


**55** **56** **57**

Because of the failure of these cyclization reactions and the difficulties associated with using HF, yet another approach to this system was explored in which 4-chloro-1-methylpyridinium iodide (**58**) was allowed to react with indazole (**44**) with the hope of generating the pyridinium products **48** and **49** (**Scheme 15**). This approach is similar to that described in **Scheme 11** with the obvious advantage of avoiding the need for 4-fluoropyridine as a reactant.

**Scheme 14: Formation of** 48

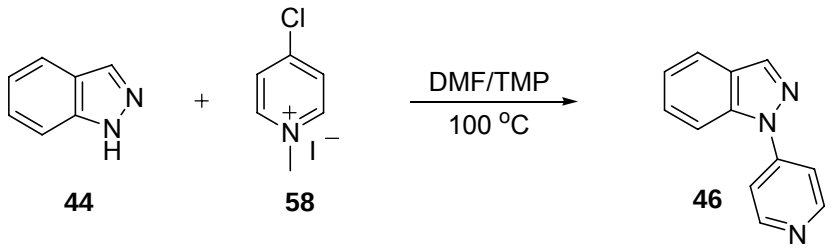


**44** **58**

After heating the reactants for 24 hrs in DMF, GC-EIMS analysis demonstrated that the starting materials had been consumed. As was expected, the GC-EIMS displayed the demethylated pyridine compound **46** that would be formed following thermal demethylation of **48** in the GC inlet (see below). However, workup of the reaction mixture provided evidence that **46** was present in the reaction mixture itself. This suggested that thermal N-demethylation had occurred during the course of the reaction. Furthermore, only the 1*H*-isomer was detected by GC-EIMS. This observation will be discussed in more detail later.

Since the reaction described in **Scheme 14** gave only the demethylated product, more gentle reaction conditions (22 ˚C rather than 100 ˚C) were examined (**Scheme 15**).

**Scheme 15: Formation of** 48 **and** 49

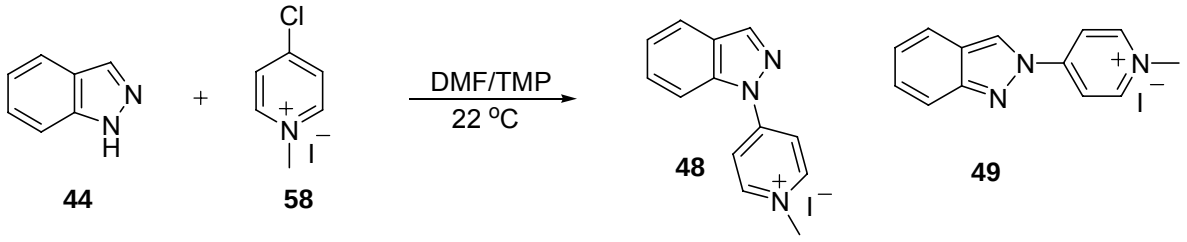


**44** **58** **48** **49**

The reaction (**Scheme 15**) gave the desired 1*H*- and 2*H*-methylated isomers in a 3:1 ratio and established that the high temperatures used earlier are unnecessary. This behavior could be documented by both HPLC and GC-EIMS. The 1*H*-isomer, which crystallized during the course of the reaction, was easily separated from the reaction mixture by filtration while the 2*H*-isomer remained in solution. When the reaction described in **Scheme 15** was run at reflux, only the 1*H*-isomer was formed. This

suggested that the 2*H*-isomer was undergoing a rearrangement process under these conditions. Moreover, it is difficult to get the 2*H*-isomer in large amounts with this reaction, which produces principally the 1*H*-isomer. A different approach for obtaining the 2*H*-isomer will be discussed later. The reason the primary product above is the 1*H*-isomer is because the electron pair of the anion **59a ↔ 59b** is localized primarily on N(1) which retains the intrinsic aromatic character of the benzene ring.

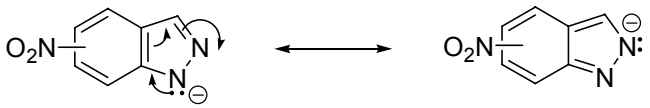

**59a** **59b**

In the past, the synthesis of the 2*H*-isomers was attempted in the absence of base. The reaction was thought to give the 2*H*-isomer via the intermediate described below. Substitution at the 2-position gives a resonance-stabilized cation (**60a ↔ 60b**) whereas substitution at the 1-position (**61**) does not yield a resonance-stabilized product. The reaction was tried in DMF and only the 1*H*-isomer was obtained. One of the current goals within this present study is to synthesize these *2H*-isomers.

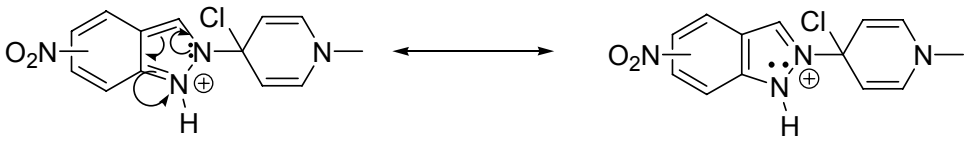

**60a** **60b**

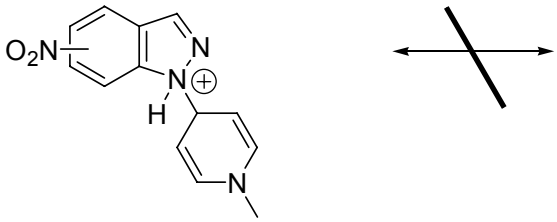

**61**

## 3.0 Accomplishments

### 3.1 Chemistry

Studies by Isin have established that nucleophilic aromatic substitution between 1-methyl-4-chloropyridinium iodide (**54**) and various nitroindazoles in the presence of base leads primarily to the formation of the *1H* isomers.[1] We have examined this reaction with 5- and 6-nitroindazole and obtained identical results. The purpose of resynthesizing the known compounds was to have material to re-investigate the MAO properties of the resulting 1*H*-prodrugs. Another goal of the current study was to synthesize the *2H*-isomers (**62** and **63**) as precursors to the desired prodrugs **30** and **32**. These two prodrugs were previously unattainable but were needed to compare their MAO properties with the other known regioisomers. Furthermore, we wanted to synthesize a prodrug that would release the parent compound upon bioactivation. Success in this effort could provide an opportunity for an *in vivo* neuroprotection study. This activation, seen previously in the benzimidazole series,[48] has not been observed as an efficient reaction in the indazolyl series. As a result, we wanted to synthesize and test the MAO substrate properties of **30** and **32** together with the regioisomeric benzimidazole **64** in the hope of seeing the anticipated hydrolytic cleavage of the MAO–generated dihydropyridinium metabolites.

[48] References 45 and 46

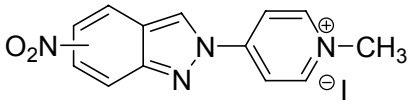

**62**, 5-$NO_2$
**63**, 6-$NO_2$

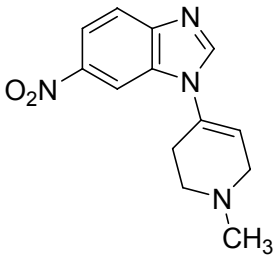

**64**

### 3.1.1 Synthesis and Characterization of the 2*H*-Prodrugs of 5- and 6-NI

Earlier attempts to prepare the *2H*-regioisomers of 5- and 6-nitroindazolyl prodrugs **30** and **32** involved the condensation of the nitroindazoles with 4-chloro-1-methylpyridinium iodide (**58**). The reactions were carried out in DMF in the absence of base. These efforts failed, apparently because of the high-energy barrier leading to the proposed intermediates (**65** and **66**).

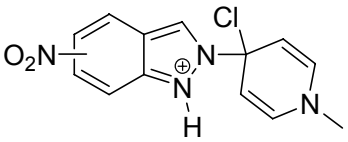

**65**, 5-$NO_2$
**66**, 6-$NO_2$

More vigorous conditions were explored by running the reactions in the absence of DMF, with the nitroindazoles **16** and **17** as 'solvents'—that is, the reactions were carried out in a meld. The preliminary trial of this experiment was done in a melting point apparatus. For this initial experiment, the reaction was carried out using a 1:1 ratio of the nitroindazoles (**16** and **17**) to the 4-chloro-1-methylpyridinium iodide (**58**). For the preparative scale synthesis of **62 (Scheme 16**), the mixture was heated to 180 °C to achieve the meld (see below). After cooling the test tube containing **16** to room temperature, TLC analysis documented that the starting indazole reagent (**16**) had been

consumed and that a new product, presumably the desired condensation product, **62**, had formed. Since this initial experiment was done with such small amounts of materials, not enough product was available for full characterization.

**Scheme 16:** Formation of **62**

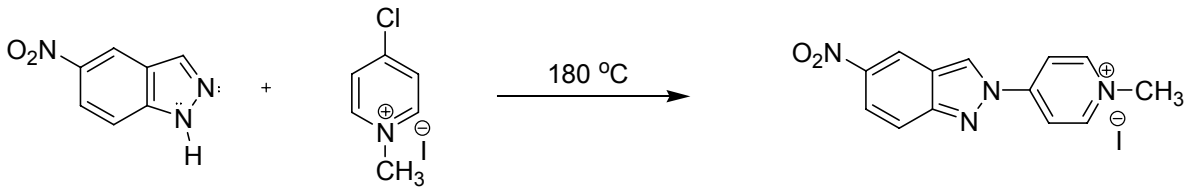


**16** **58** **62**

The reaction was run on a larger scale to obtain a sufficient amount of product for characterization. The scaled up reaction was attempted initially with a 5:1 ratio of nitroindazoles (**16** and **17**) to pyridinium **58**. The reactions were repeated several times, varying the ratio of nitroindazoles (**16** and **17**) to pyridinium **58** and the yields were consistently below 30%. Finally, a ratio of 1:1 proved to be as effective as the original 5:1 ratio reaction and resulted in easy isolation as less starting material was present in the crude product. The $^{1}$H NMR spectrum (Fig. 2) of the product isolated from the reaction of **16** and **58** confirmed the presence of a single isomer.

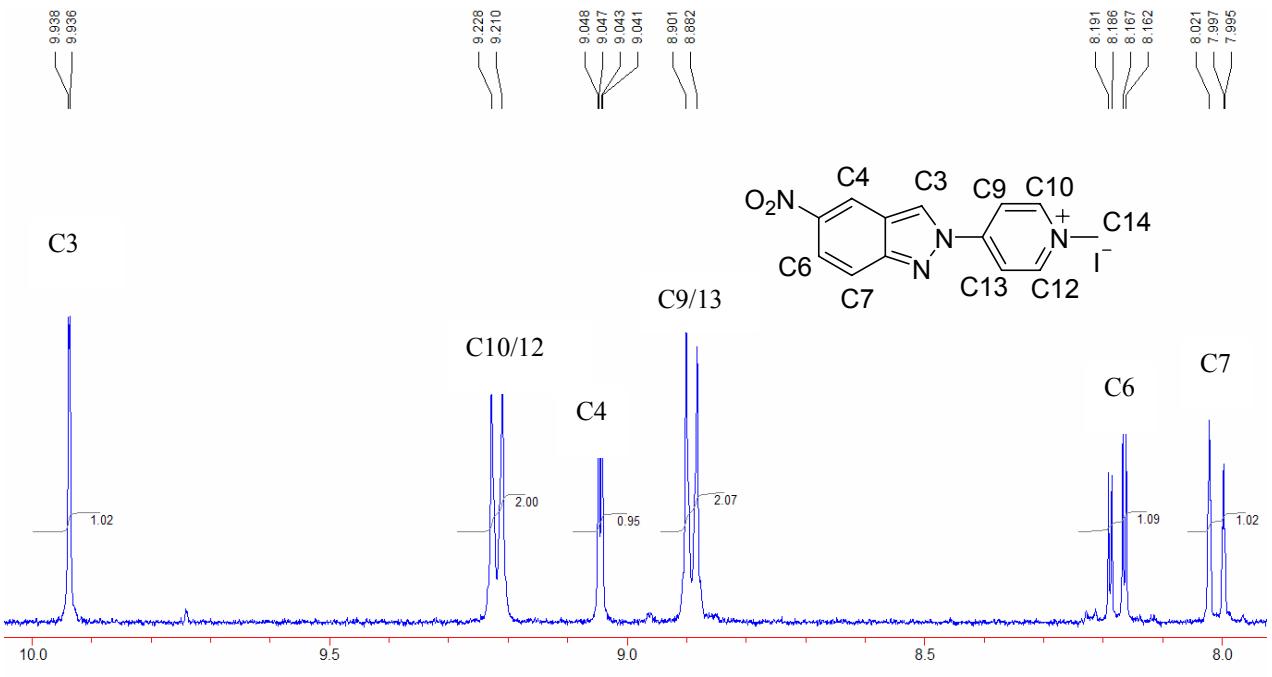


**Figure 2. $^{1}$H NMR spectrum of 62**

We performed a NOESY experiment in order to document through space $^{1}$H-interactions revealed by the Nuclear Overhauser Effect (NOE). When one proton signal is irradiated, the intensities of nearby nuclei are affected. For the 1*H*-isomer, one should observe an NOE interaction between C9/C13 and C7. In fact, we observed that the protons at C9/C13 had through space interactions with the proton on C3 (Fig. 3) of the molecule. This result established that the product obtained was the desired 2*H*-isomer **62**. This NOESY spectrum also identified the $^{1}$H-interaction between C10/12 and C14.

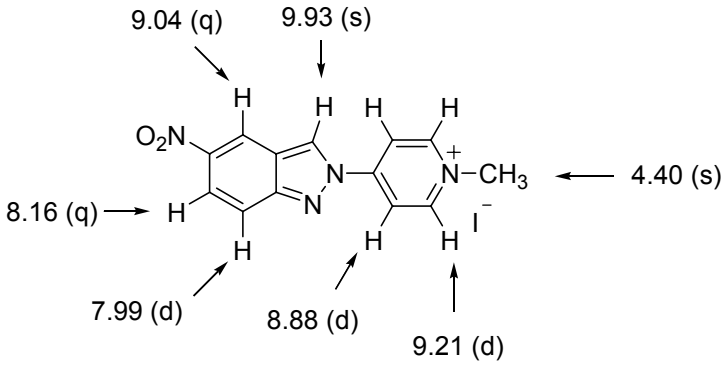


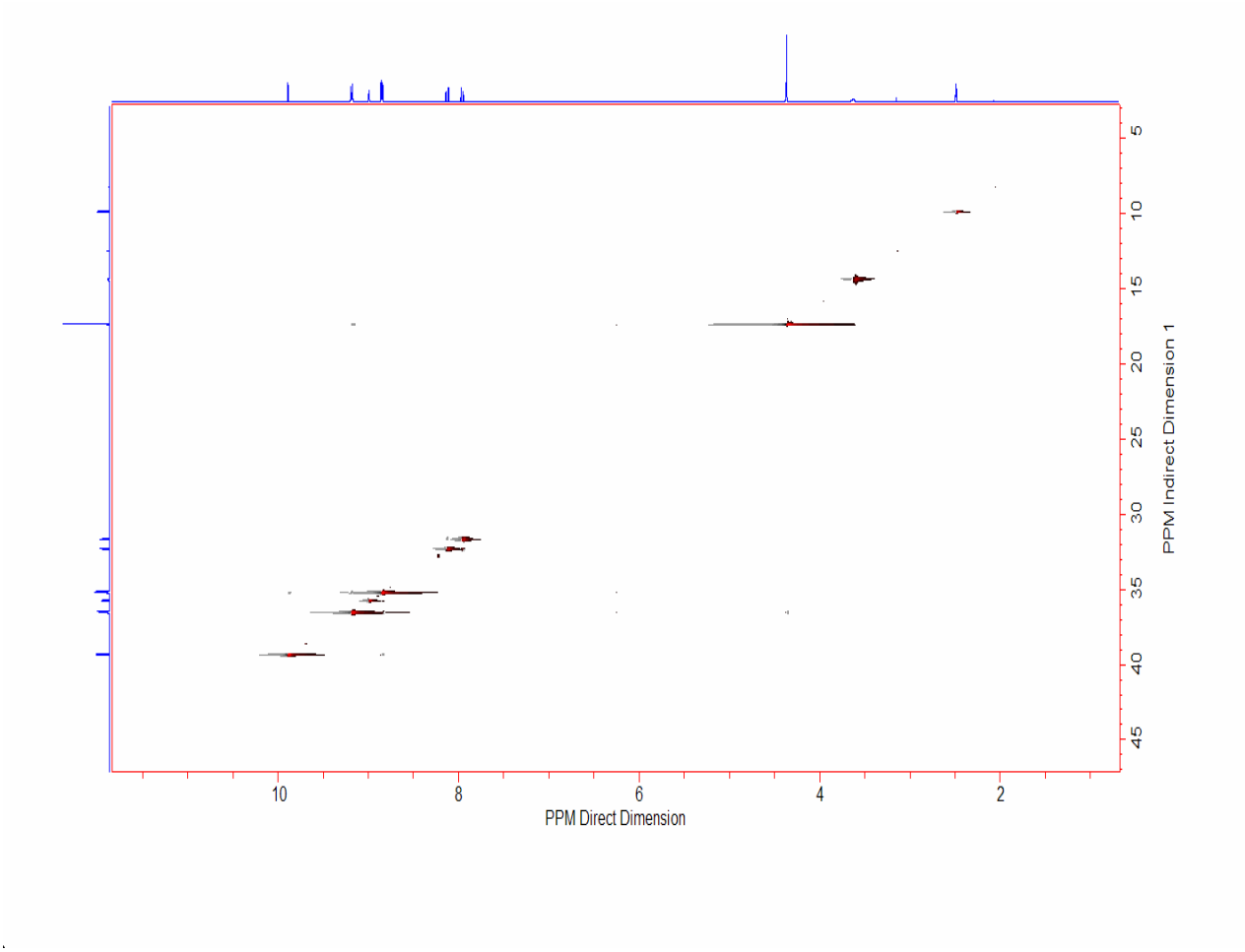


**Figure 3. NOESY spectrum of 62**

The formation of **62** is consistent with a pathway in which the charged intermediate (**65**) in this condensation reaction is formed.

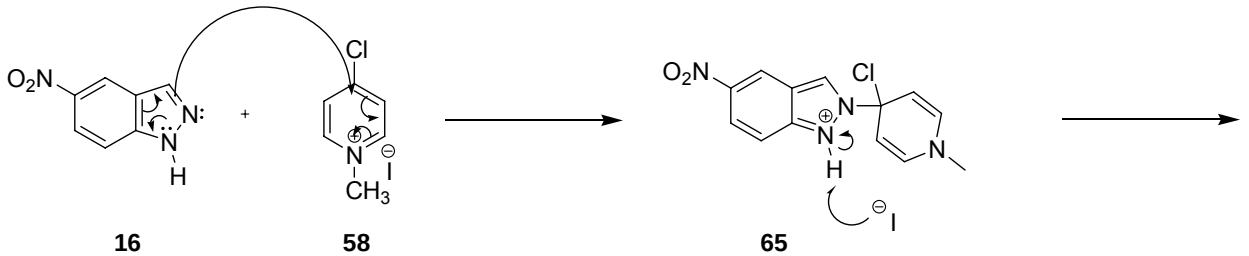

**16** **58** **65**

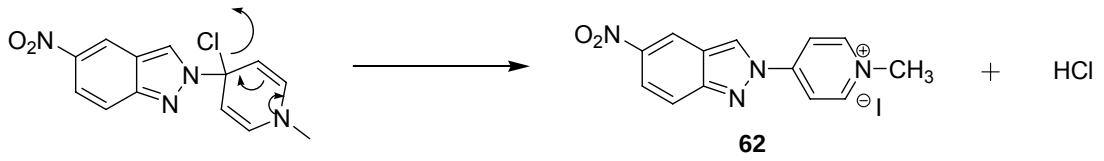

**62**

The same procedure was followed with **17** and **58** to synthesize the 2*H*-isomer **63**. Identical results were obtained for this 2*H*-isomer as for **62**. Finally, the compounds were submitted for C, H, and N analysis to Atlantic Microlab, Inc. The results established that carbon was off by ~50%. After some speculation, we realized that the compounds obtained were not the iodide salts but rather the triiodide salts (**67** and **68**). An iodine analysis confirmed this conclusion. The formation of the $I_3$ counterion was not investigated any further.

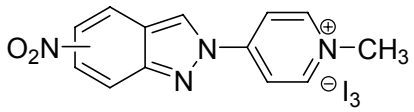

**67**, 5-$NO_2$
**68**, 6-$NO_2$

These pyridinium products were treated with $NaBH_4$ to give the desired 2*H*-prodrugs. These two tetrahydropyridines (**30 and 32**) were converted into their oxalate salts with oxalic acid in ether.

### 3.1.2 Synthesis and characterization of the 6-NBI prodrug 64

Another compound of interest was the regioisomer **64** that should be generated with the nitrobenzimidazole **23.** Regioisomer **43** was already available (see Section 2.8). The synthesis of prodrug **64** was attempted with the two-step reaction pathway shown in **Scheme 17**. The condensation reaction between **23** and **58** was carried out in DMF at 70 °C in the absence of base. The reaction mixture was cooled to room temperature and the product was collected by filtration. NMR analysis indicated that the condensation reaction led to a mixture of products, presumably 1-methyl-4-(5-nitrobenzimidazolyl)pyridinium iodide (**69**) and 1-methyl-4-(6-nitrobenzimidazolyl) pyridinium iodide (**70**).

**Scheme 17:** Formation of **43** and **64**

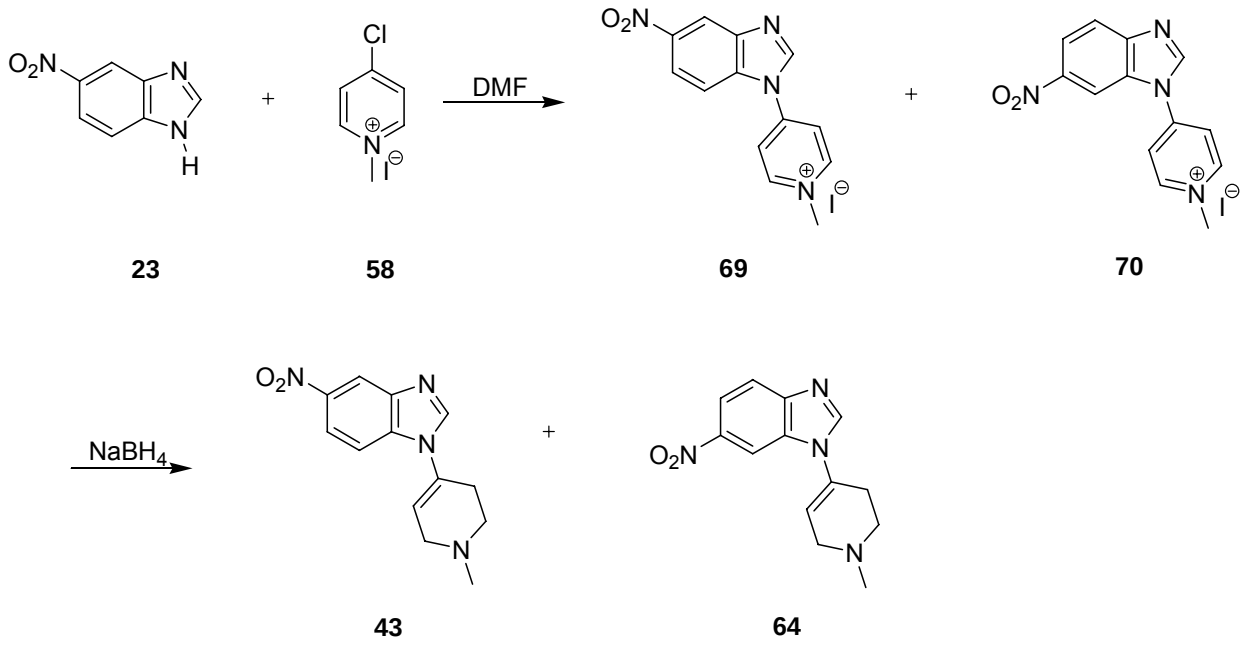


**23** **58** **69** **70**

**43** **64**

The products **69** and **70** were obtained as a 1:1 ratio based on the crude NMR spectrum. Following recrystallization, the mixture was enriched with one isomer. The NMR of this isolate is shown in **Figure 4**. Further attempts to purify the enriched pyridinium product were unsuccessful so we proceeded to the next step for the synthesis of prodrug **64** with the mixture.

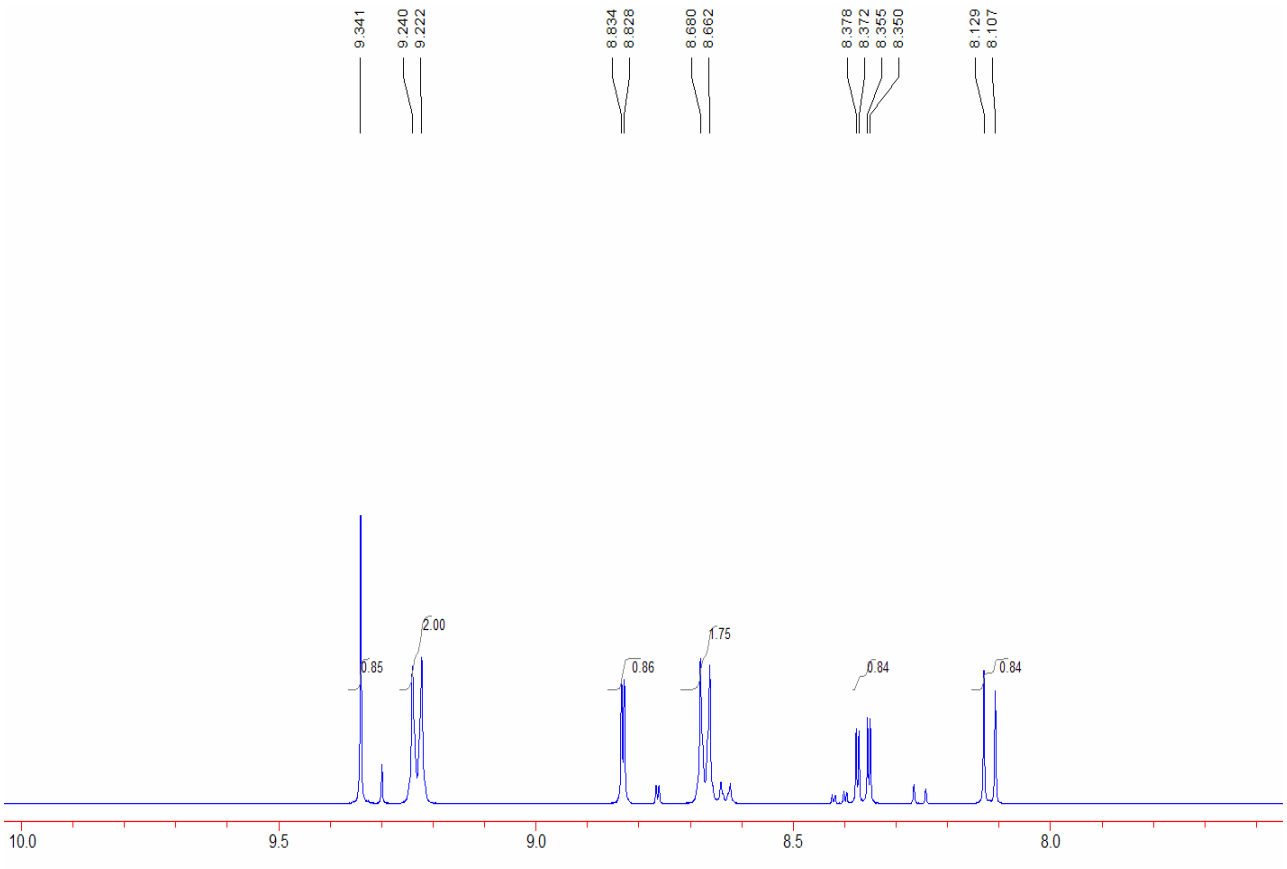


**Figure 4. $^{1}$H NMR of the 1$^{st}$ step product from Scheme 16**

This enriched isolate of pyridinium species was reduced with $NaBH_4$ in methanol. The GC/MS of the reaction mixture confirmed the conversion into the anticipated tetrahydropyridinyl products ($M^{\bullet+}$ at *m/z* = 258) **43** and **64** shown in **Scheme 17**. Treatment with oxalate acid followed by recrystallization led to the isolation of the oxalate salt of one regioisomer the structure of which needed to be established.

The $^{1}$H NMR of the isolated oxalate salt is shown in **Figure 5**. We assigned the most downfield signal ($\delta$ 8.77 ppm) to the proton on C2. It is attached to an sp$^{2}$-hybridized atom and is expected to be less shielded. Furthermore, the peak is a singlet indicating

the absence of an adjacent C—H system. The next most upfield signal at δ 8.52 ppm was assigned to the proton on C7 of **64**. It is a doublet and shows *meta* coupling (*J* = 2 Hz). This would correspond to C4 of **43**. The quartet at δ 8.14-8.16 ppm was assigned to the proton on C5 of isomer **64**. It shows *ortho* (8.4 Hz) and *meta* (2 Hz) coupling resulting from the interactions with the C7 and C4 protons. The quartet at δ 8.14-8.16 could also be assigned to the proton on C6 of isomer **43**. The final aromatic proton at C4 of **64** was assigned to the doublet at 7.9 ppm. It displays *ortho* coupling (9.2 Hz) because of its interaction with the proton on C5 of isomer **64**. This could represent the C7 proton of **43**.

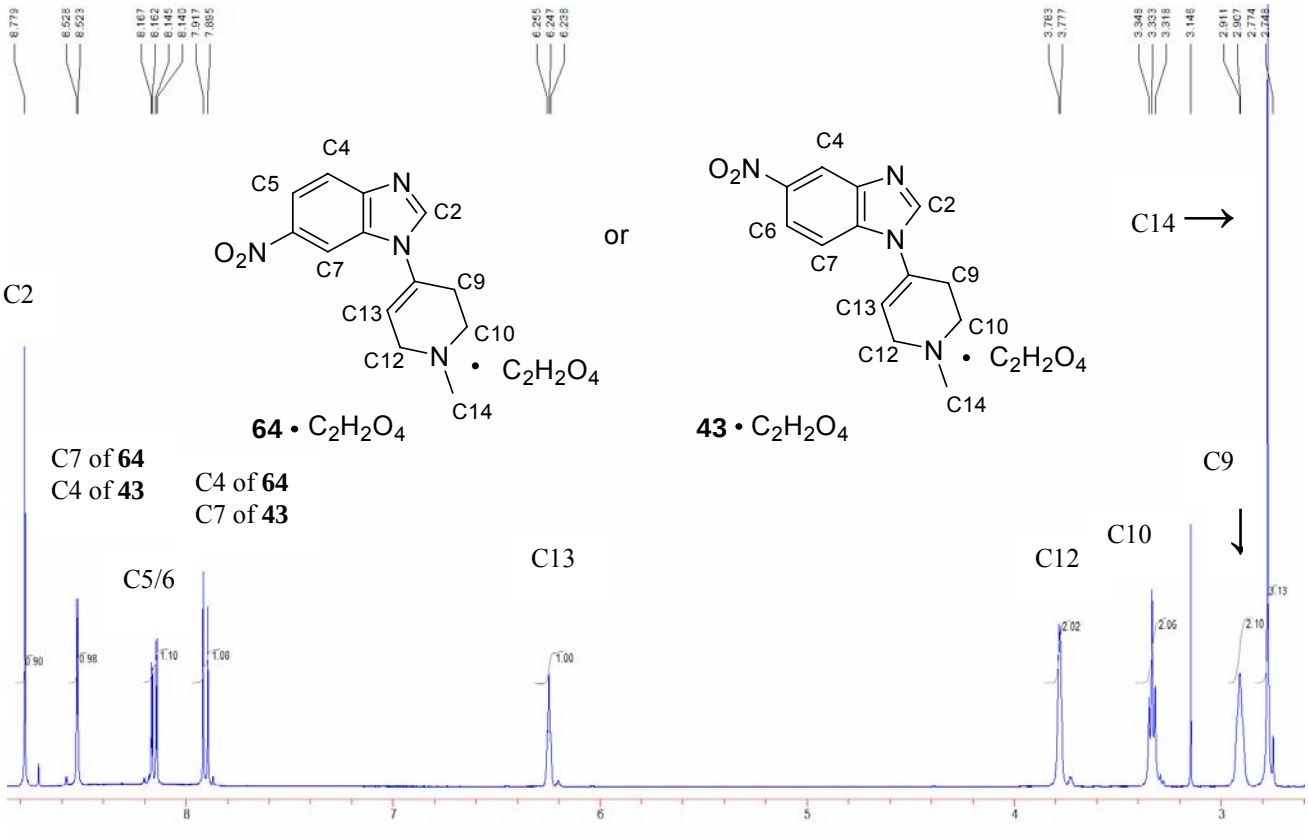


**Figure 5. $^{1}$H NMR of product from 2$^{nd}$ step of Scheme 16**

Based on the spectrum, it was apparent that the pyridinium moiety had been replaced with a tetrahydropyridinyl moiety, as expected. However, the spectrum did not lead to an unambiguous regiochemical assignment. In order to make this assignment, a NOESY experiment was conducted (**Fig. 6**). If the product were the 5-nitro regioisomer, a $^{1}$H-interaction between C13/C9 would be seen with a proton that shows *ortho*-coupling, like the C7 proton of **43**. However, we see an interaction between the C13-proton and the *meta*-coupled proton on C7 indicating that the product is the 6-nitro regioisomer **64**.

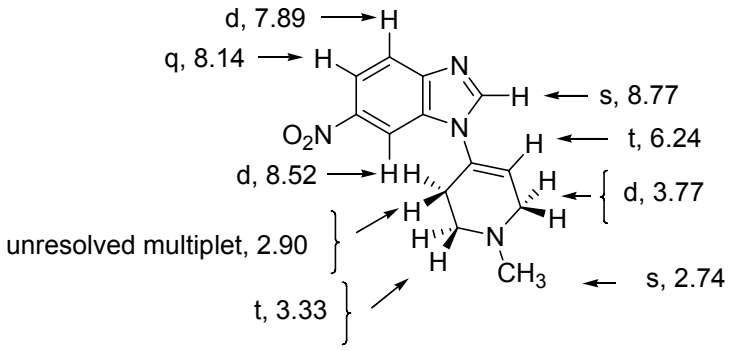


**64** • $C_2H_2O_4$

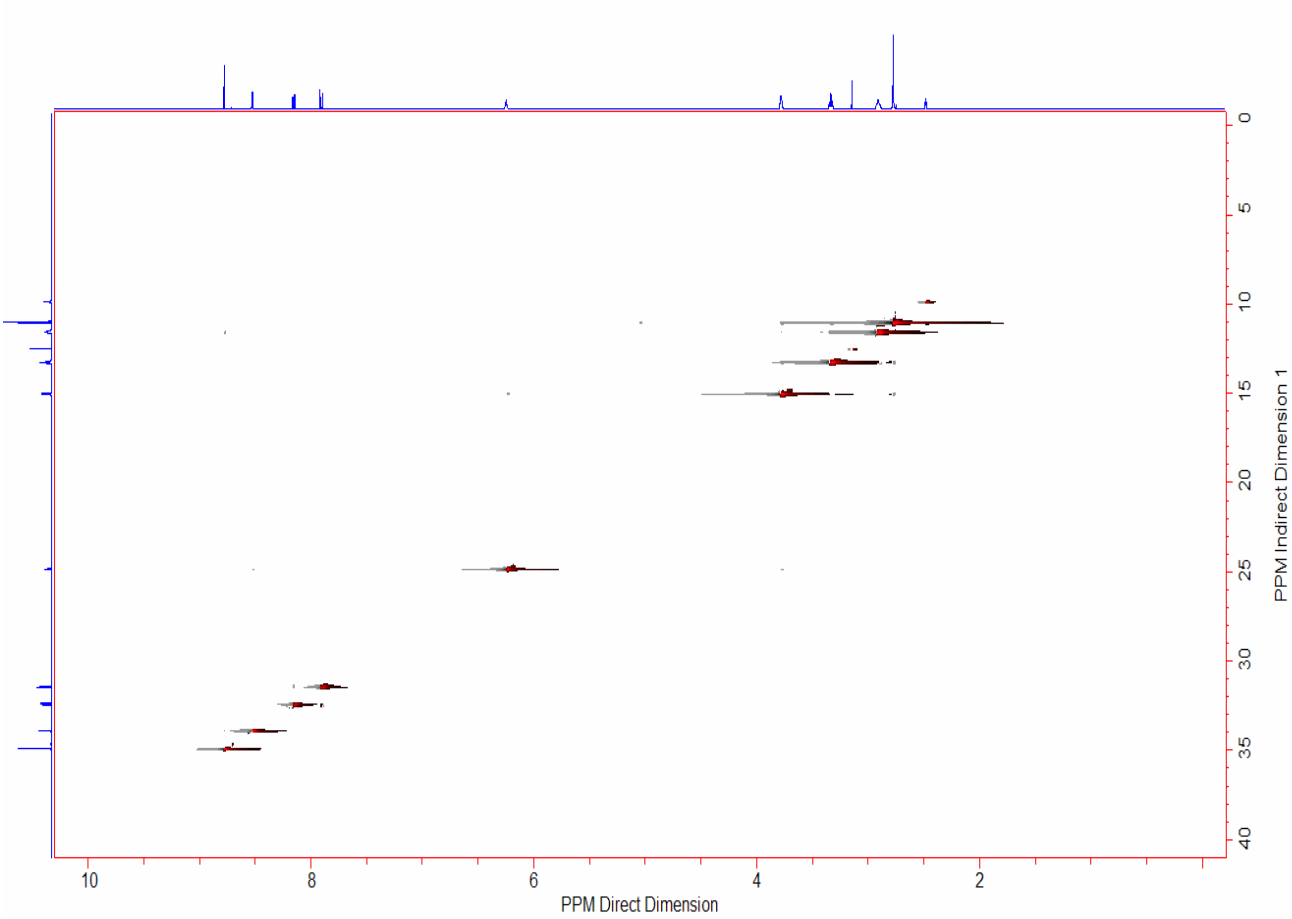


**Figure 6. NOESY spectrum of 64.**

### 3.2 Biology

The tetrahydropyridinyl prodrugs **29** and **31** of 5- and 6-nitroindazole, **16** and **17**, respectively, are known substrates of MAO.[49] They undergo initial oxidation to give the corresponding dihydropyridinium intermediates **37** and **38** (**Scheme 18**). After this activation step, the intermediates may be further oxidized to the pyridinium species (**40** and **41**) or may undergo hydrolytic cleavage to release the parent indazoles (**16** and **17**). The metabolically generated dihydropyridinium products, however, do not undergo

[49] Reference 1 and Reference 46

hydrolytic release of parent compound.[1] As discussed above (**Scheme 10**), the problem may be related to the requirement for the formation of the high energy 2*H*-tautomer.

Benzimidazolyl prodrugs **35** and **43** have both been shown to release the parent benzimidazole upon MAO-B bioactivation in *in vitro* bioassays. This interesting characteristic of the benzimidazolyl prodrugs could prove to be valuable in that it may lead to release of an active inhibitor of MAO-B in the brain where MPTP undergoes MAO-B-catalyzed bioactivation.

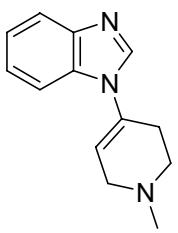

**35**

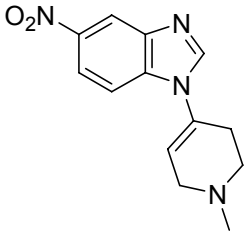

**43**

We have studied the interactions of **29-32** and **64** (**Scheme 17**) with MAO-A and MAO-B. The *in vitro* studies were designed to also provide additional information regarding the active sites of the enzymes which will be discussed later.

**Scheme 18:** MAO oxidation of **29**-**32** & **64**

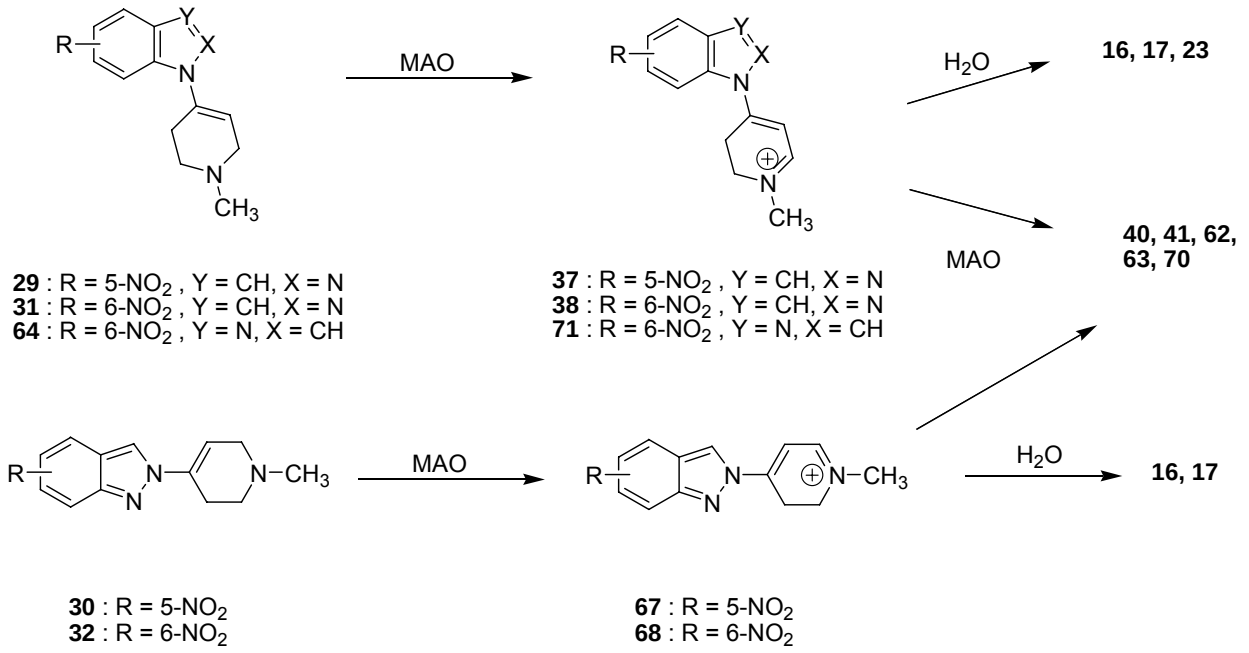


### 3.2.1 Reinvestigation of the *1H*-5-NI (29) and 1*H*-6-NI (31) Prodrugs with MAO

The 1*H*-prodrugs **29** and **31** of 5- and 6-NI, respectively, were tested for their MAO substrate properties to document that our assay would provide results comparable to those already reported and to provide a systematic set of data.[1] The compounds were initially examined by incubating the prodrug (160 µM) with the enzyme preparation (0.3 mg/mL). The enzyme source for MAO-B was baboon liver mitochondria while the enzyme source for MAO-A was human placenta mitochondria. Following the incubation period, the protein was sedimented by the addition of acetonitrile and the supernatant fractions were analyzed by HPLC-UV/Vis-DA (Diode array) to record the formation of metabolites as well as the decrease in substrate concentration. To ensure that the metabolites formed were from the enzyme-prodrug interaction, a control experiment was conducted in the absence of enzyme. No metabolite formation was observed.

### 3.2.1.1 MAO Properties of 1*H*-5-NI prodrug (29)

Compound **29** (160 μM) showed good substrate properties with MAO-B (0.3 mg/mL) as its concentration decreased to ~15% after a 120 minute incubation period (**Figure 7**).

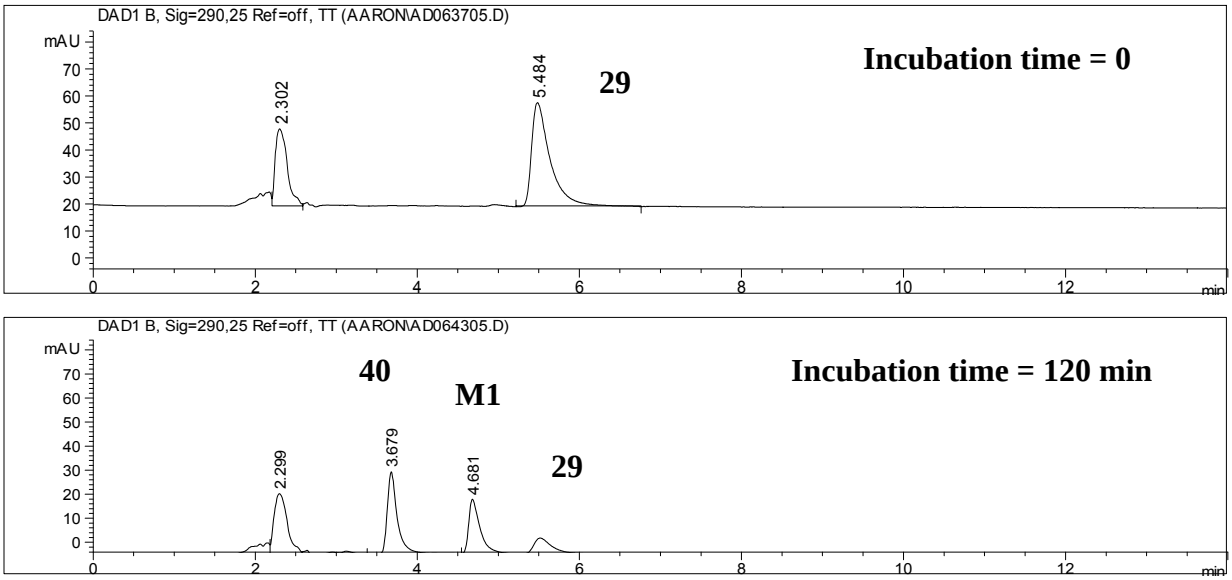


**Figure 7. HPLC analysis of supernatants from the incubation of 29 with MAO-B**

Nevertheless, it was observed that no metabolism-dependent release of the parent indazole (**16**) had taken place. Instead, the prodrug **29** is oxidized to the pyridinium product **40** as reported.[1] This was confirmed by a comparison of the UV spectra for the enzymatically formed pyridinium species with a synthetic sample of **40** (**Figure 8)**.

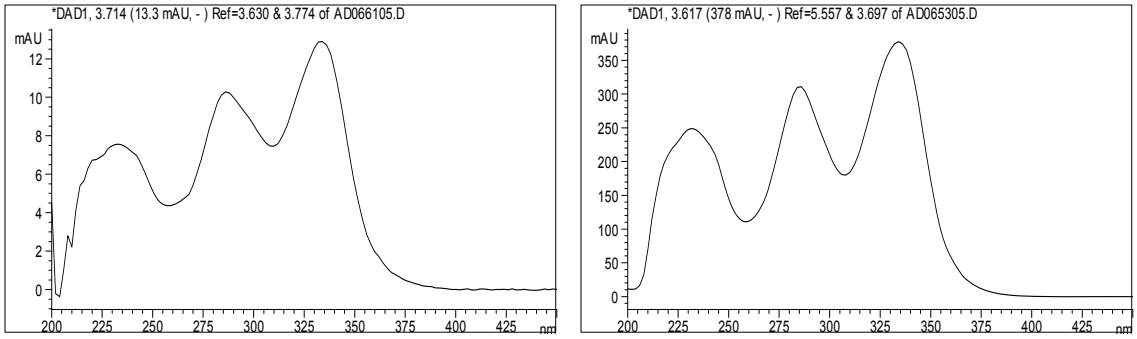


**Figure 8. UV spectra of 40. Synthetic (right) and Enzymatic (left).**

The other metabolite, which was also observed before but had not been characterized, is labeled as **M1** (**Figure 7**). A possible structure for this unknown metabolite is the dihydropyridinium species **37**, the initial oxidation product of **29** (**Scheme 18**).

**Scheme 19:** MAO-catalyzed oxidation of **29**

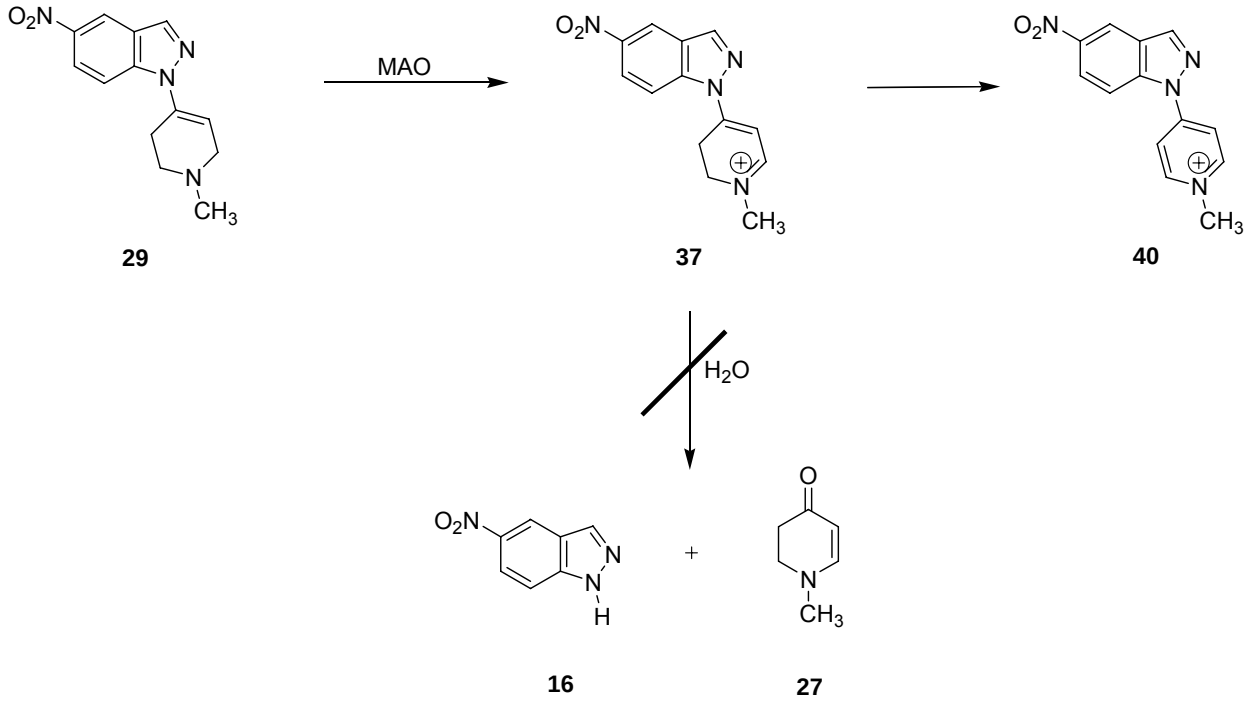


**29** **37** **40**

**16** **27**

The corresponding HPLC-UV/Vis-DA analysis of the fate of 5-NI 1*H*-prodrug **29** (160 μM) in the presence of MAO-A (0.3 mg/mL) provided a different picture from that reported previously.[1] In the present study, the substrate concentration decreased ~ 60% after 60 minutes compared to the 20% reported earlier. Furthermore, the two metabolites (**40** and **M1**), previously reported as minor products, were much more abundant. The reason(s) for the difference is (are) not apparent. The HPLC-UV/Vis-DA tracings of the incubation mixtures obtained with **29** and MAO-A are shown below (**Figure 9**).

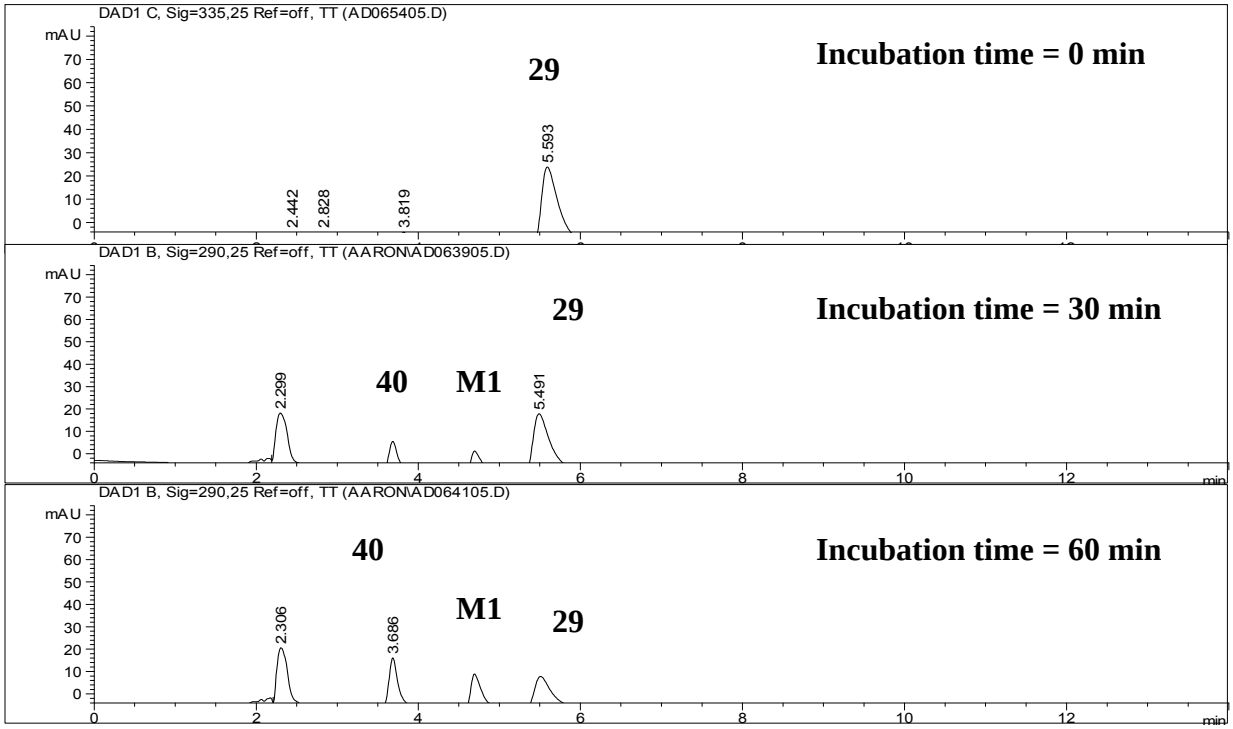


**Figure 9. HPLC analysis of supernatants from the incubation of 29 with MAO-A**

### 3.2.1.2 MAO Properties of the 1*H*-6-NI prodrug 31

Compound **31** was also reevaluated for MAO substrate properties. Based on the HPLC tracings, it was apparent that **31** (160 μM) is not as good a substrate for MAO-B (0.3

mg/mL) as is **29**. This was apparent since the substrate concentration decreased by only 5% after a 120 minute incubation period (**Figure 10**).

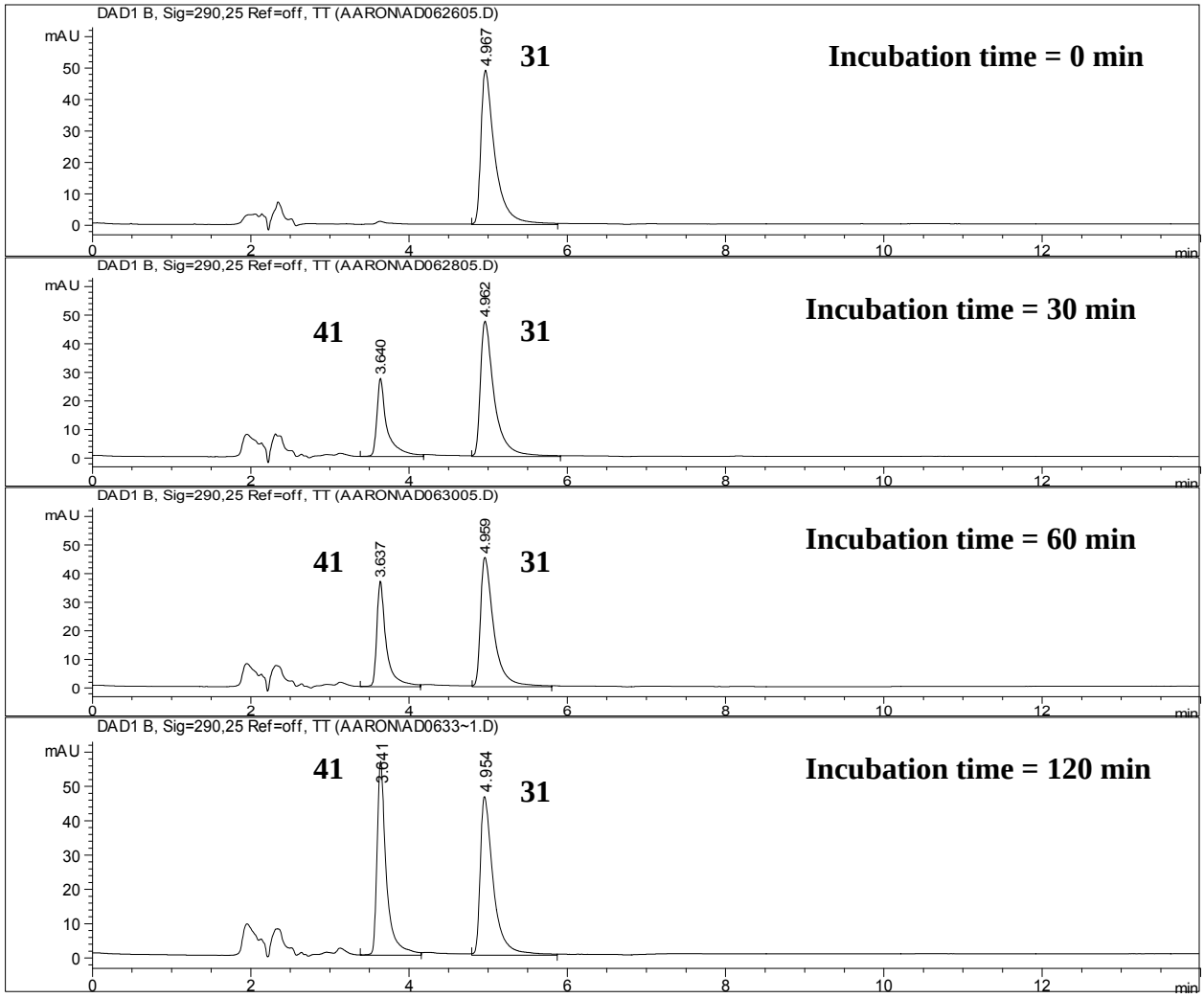


**Figure 10. HPLC analysis of supernatants from incubation mixtures containing 31 and MAO-B.**

The MAO-B-catalyzed reaction led to the formation of the pyridinium species **41** as the major metabolite (**Scheme 20**). This was confirmed by comparing the UV spectra of the synthetic pyridinium species with the enzyme-generated metabolite (**Figure 11**). Again, this is analogous to what was observed previously with the 1*H* isomers.[1]

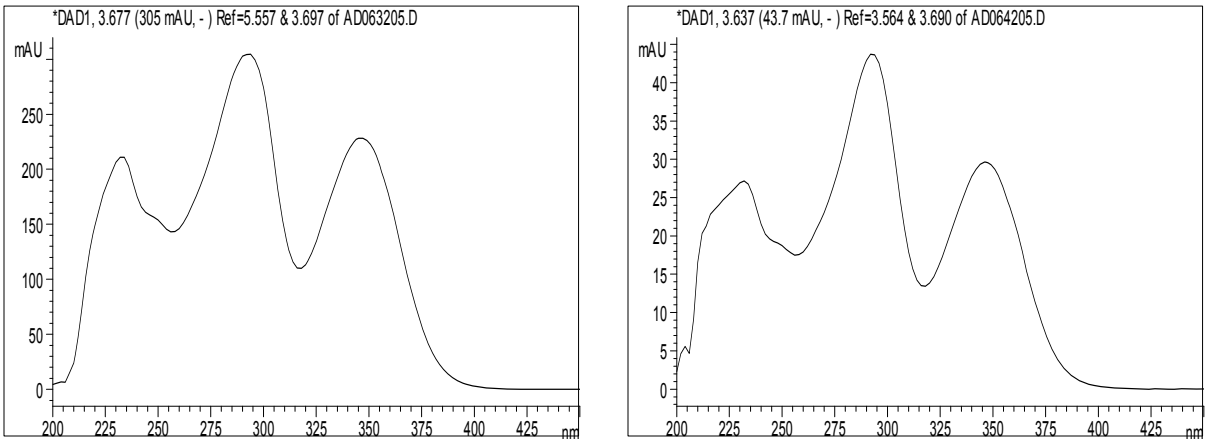


**Figure 11. UV spectra of 41. Synthetic (left) and Metabolite from Figure 10 (Right).**

**Scheme 20:** MAO-catalyzed oxidation of **31**

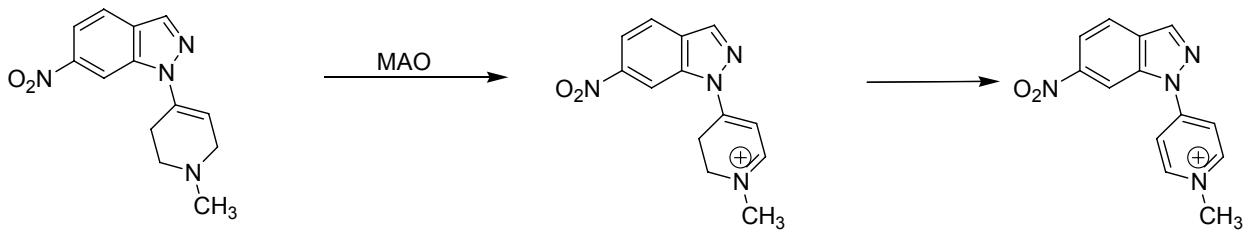


**31** **38** **41**

The Michaelis-Menten kinetic values ($K_m$ and $V_{max}$) with MAO-B had not been determined for this compound and are reported below (**3.2.1.3**). We have also repeated the studies of **31** with MAO-A and found similar results upon MAO-A activation to those reported previously.[1] The results from this study are presented in **Figure 12**.

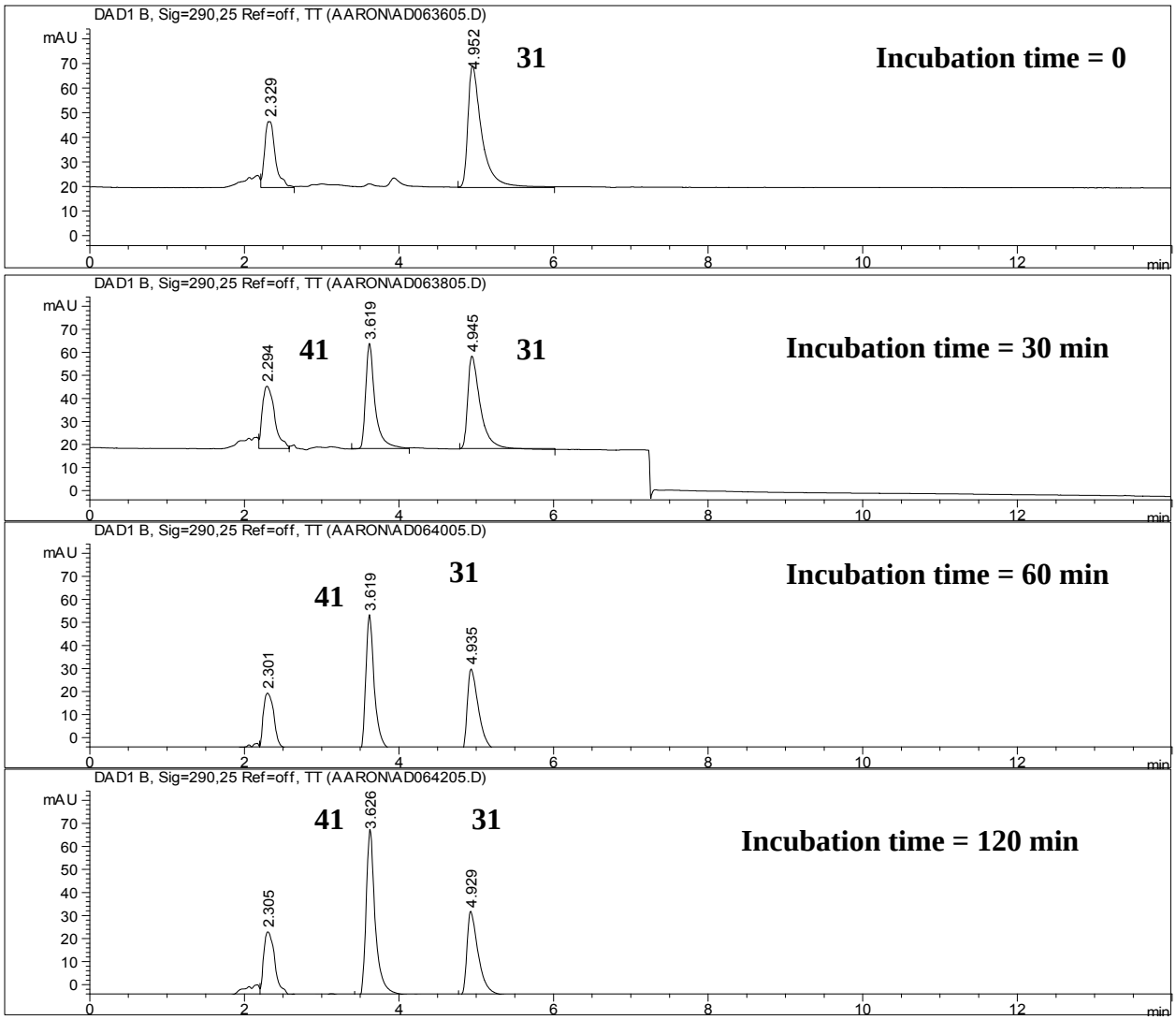


**Figure 12. HPLC analysis of supernatants from incubation mixtures containing 26 and MAO-A.**

### 3.2.1.3 Investigation of the 6-NI 1*H* prodrug 31 kinetics with MAO-B

After confirming that **31** was a substrate for MAO-B, it was decided to determine the kinetic values ($K_m$ and $V_{max}$) for this oxidation. A series of tubes containing various concentrations of the 6-NI 1*H* prodrug substrate were prepared. Over the course of 60 minutes we measured the extent of formation of the pyridinium metabolite **41**. The initial

velocities ($V_i$) were determined during the first 15 minutes of the reaction when the substrate was in substantial excess. These values (rates) were determined by taking the slopes of the linear series of plots as shown in **Figure 13**.

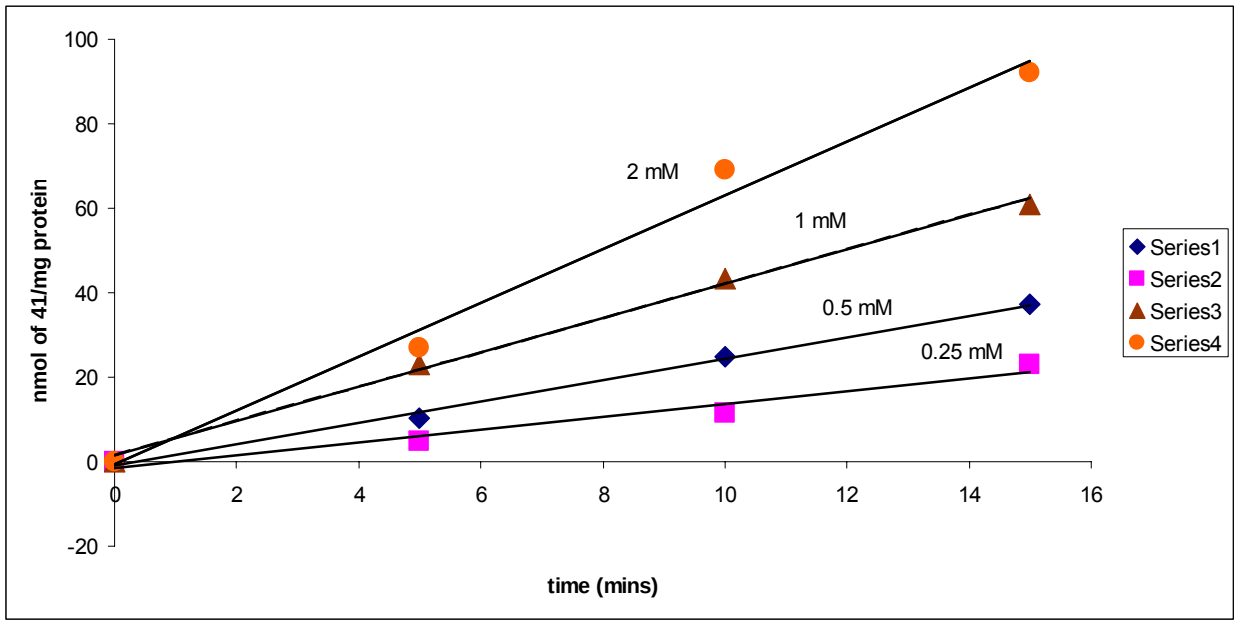


**Figure 13. Determination of $V_i$ for the formation of 41 at various concentrations of 31.**

By plotting the initial rates (obtained from the slopes of the lines shown in **Figure 13**) vs. the substrate concentration **[S]**, it is usually possible to estimate values for $K_m$ and $V_{max}$ (**Figure 14**). $V_{max}$ is the maximum velocity at which the reaction occurs. However, as shown in **Figure 14**, the curve never fully levels off at a maximum velocity meaning that $V_{max}$ had not been reached at the concentrations used. $K_m$ is the concentration of the substrate that results in $1/2$ $V_{max}$.

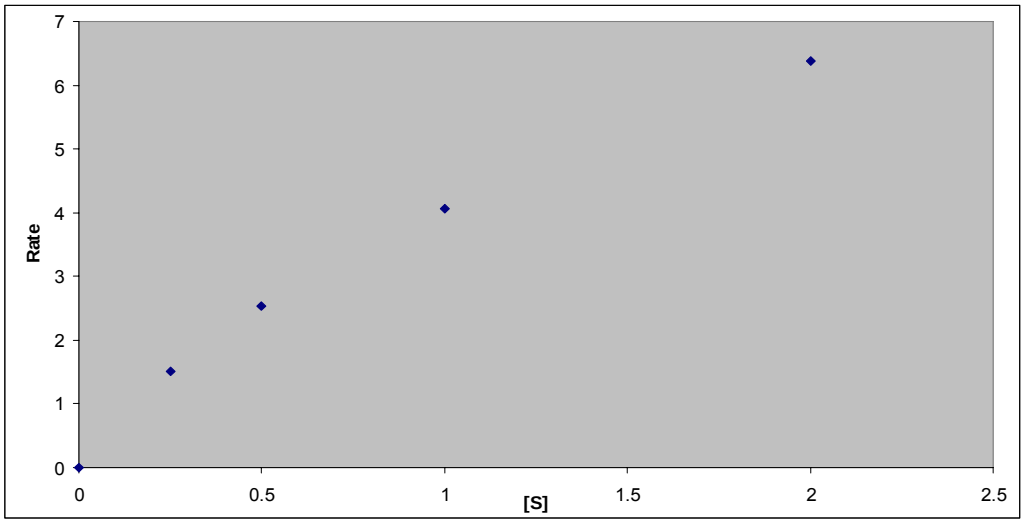


**Figure 14. Determination of $K_m$ and $V_{max}$ of 31 with MAO-B**

While it is possible to determine the kinetic values $K_m$ and $V_{max}$ from the above plot (**Figure 14**), it is easier to plot double reciprocals (1/**rate** vs. 1/[**S**]) and examine the linear series (**Figure 15**). This is called a Lineweaver-Burk plot. When x = 0, y = $1/V_{max}$. When y = 0, x = $-1/K_m$. $V_{max}$ for this reaction is estimated to be 10.2 ± 4.21 nmol/mg protein/minute while the $K_m$ is estimated to be 1.45 ± 0.39 mM.

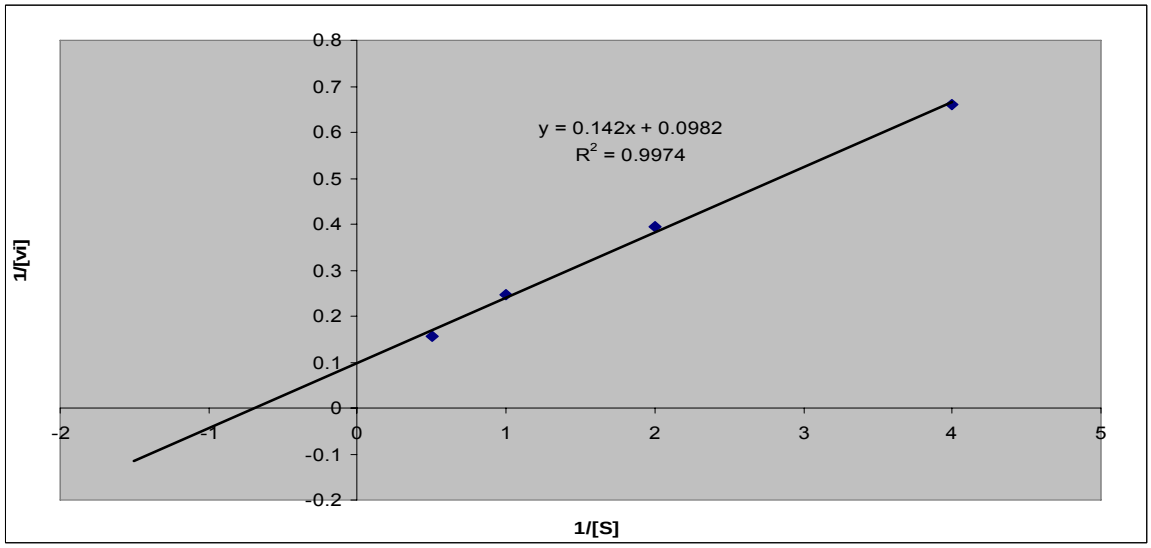


**Figure 15. Lineweaver-Burk plot prepared from data shown in Figure 13.**

### 3.2.2 Investigation of the 2*H*-5-NI (30) and 2*H*-6-NI (32) Prodrugs with MAO-B

The newly synthesized 2*H*-prodrugs of 5- and 6-NI, **30** and **32**, respectively, were also tested for MAO-B substrate properties. The final substrate and protein concentrations were 160 μM and 0.3 mg/mL, respectively. The 2*H*-7-NI prodrug **33** had already been found to not possess any MAO-B substrate properties.[1] The present results documented that both **30** and **31** were without MAO-B substrate properties. No metabolite formation was observed after a 120 minute incubation period in either case. This behavior is consistent with the active site model of MAO-B that suggests steric factors may prevent these 2*H*-isomers from fitting into the active site of MAO-B.[1]

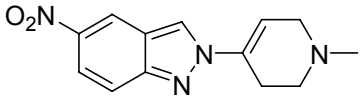

**30**

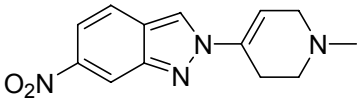

**32**

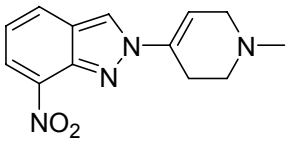

**33**

### 3.2.3 Investigation of 2*H*-5-NI (30) and 2*H*-6-NI (32) Prodrugs with MAO-A

The 2*H*-prodrugs also were examined for their MAO-A substrate properties. It has been suggested[50] that the MAO-A active site can accept larger substrates, so we anticipated that these isomeric forms of the prodrugs would be MAO-A selective because of their larger size. HPLC-UV/Vis-DA tracings obtained for the MAO-A incubation of **30** and **32** are shown in **Figures 16** and **17**.

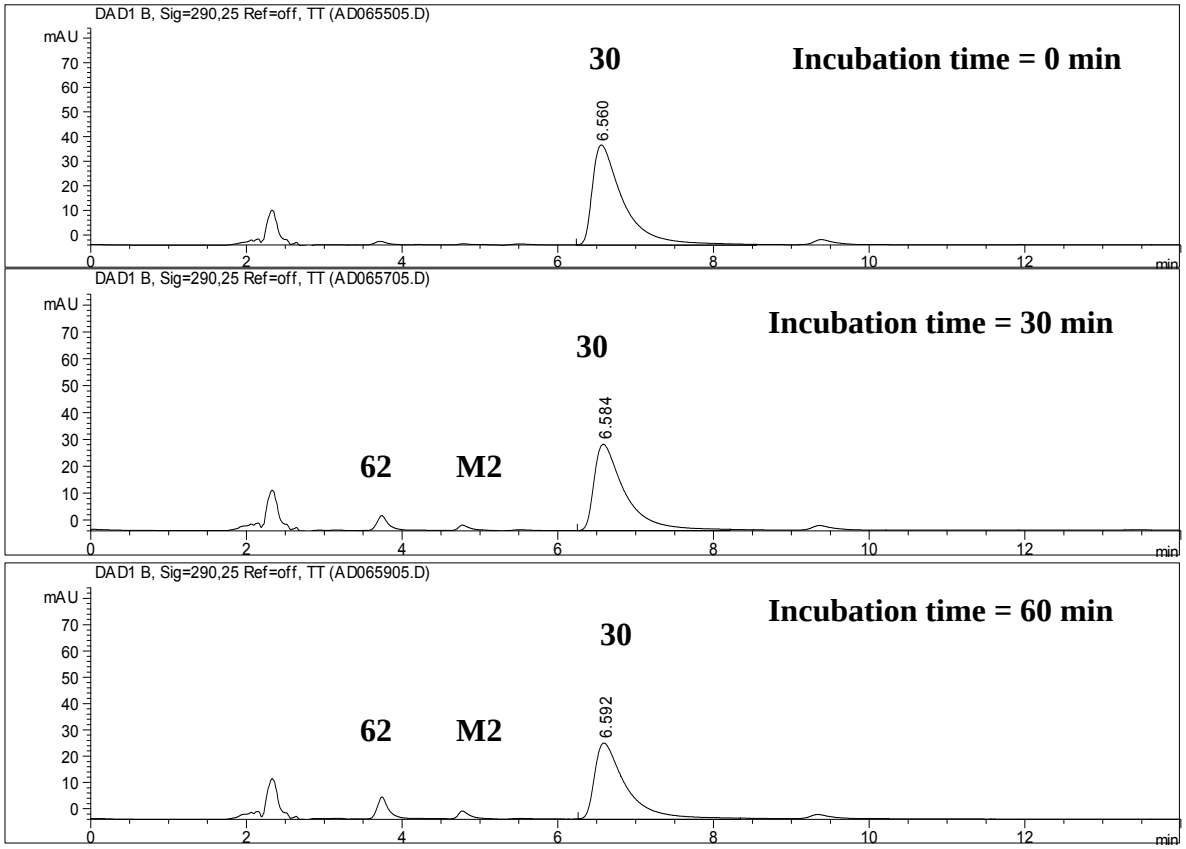


**Figure 16. HPLC analysis of supernatants from incubation mixtures containing 30 and MAO-A.**

[50] Medvedev, A.E., Ivanov, A.S., Kamyshaskaya, N.S., Kirkel, A.Z., Moskvitina, T.A., Gorkin, V.Z., Li, N.Y., Marshakov, V.Y. (1995) Interaction of indole derivatives with monoamine oxidase A and B. Studies on the structure-inhibitory activity relationship. *Biochem. Mol. Biol. Internat.* **36**, 113-122.

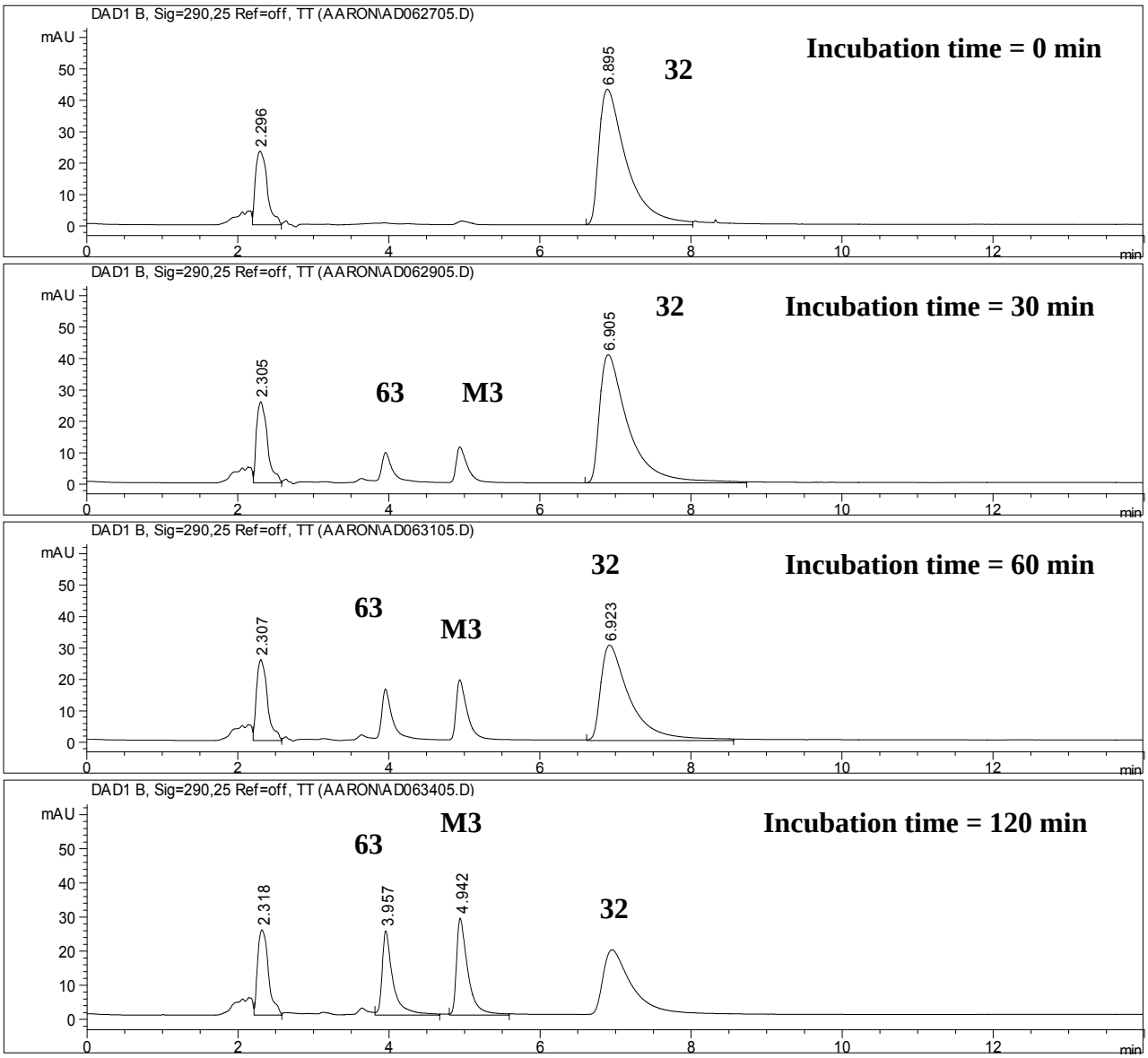


**Figure 17. HPLC analysis of supernatants from incubation mixtures containing 32 and MAO-A.**

In the case of the 5-NI 2*H*-prodrug **30**, the concentration of the substrate at t = 60 minutes showed only a moderate (~ 20%) decrease compared to the concentration at t = 0 minutes (**Figure 16**). No further significant change was seen by 120 minutes from 60 minutes for **30**. In the case of the 6-NI 2*H*-prodrug **32**, the concentration of the substrate at t = 120 minutes had decreased > 50% from t = 0 minutes (**Figure 17**). Also

seen from the tracings of **32,** the longer the incubation period, the greater the intensity of the peaks with retention times of 3.9 minutes and 4.9 minutes. Comparison of the UV-spectra of the peaks with the retention times both at approximately 3.9 minutes in each prodrug assay and of the pyridinium species **62** and **63** confirmed the predicted structures of the metabolites (**Figure 18**).

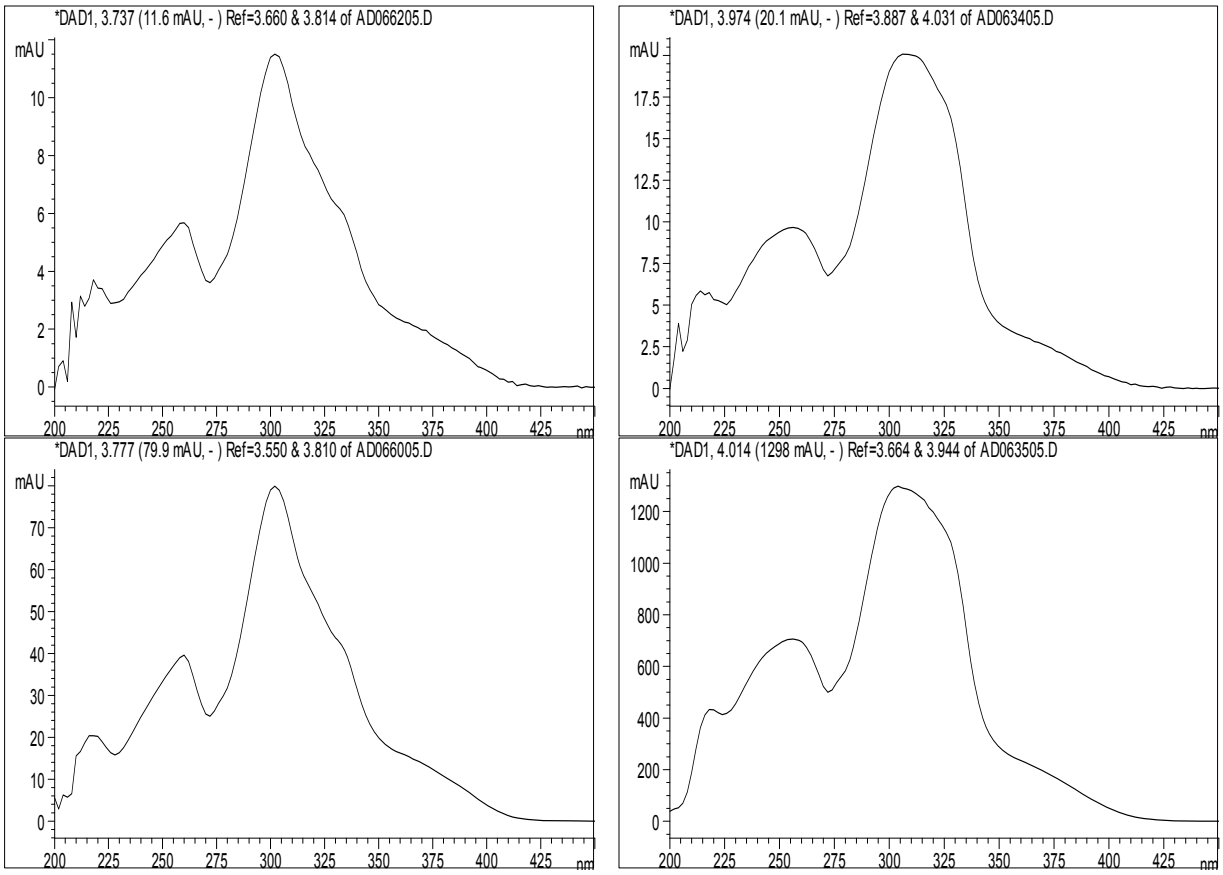


**Figure 18. UV spectra of 62 (left) and 63 (right). The synthetic standards are on the bottom while the MAO-A catalyzed products are on top.**

Both 2*H*–indazolyl prodrugs **30** and **32** showed a second metabolite as well. These are labeled **M2** and **M3** in the enzyme assay tracings, respectively. The identities of these metabolites are currently unknown. A comparison of UV spectra of **M2** and **M3** with the

indazoles **16** and **17** that would result upon hydrolysis ruled out these compounds. One possibility is that they are the corresponding dihydropyridinium species (**67** and **68**) that are formed from the initial MAO-A-catalyzed oxidation step.

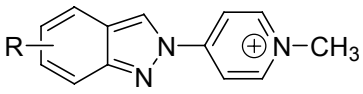

**62** : R = 5-$NO_2$
**63** : R = 6-$NO_2$

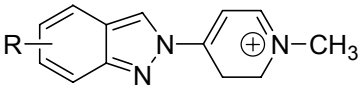

**67** : R = 5-$NO_2$
**68** : R = 6-$NO_2$

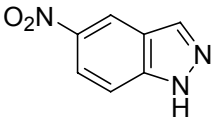

**16**

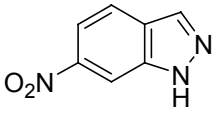

**17**

### 3.2.4 *In Vitro* Investigation of the 6-NBI Prodrug (64) with MAO-A & MAO-B

The potential prodrug 1-methyl-4-(6-nitrobenzimidazol-1-yl)-1,2,3,6-tetrahydropyridine (**64**) is expected to release 6-nitrobenzimidazole (**23**) via the mechanism shown in **Scheme 18**. The first step, which is an $\alpha$-carbon oxidation, leads to the dihydropyridinium species **71**. Hydrolysis of this intermediate will result in cleavage to release 6-nitrobenzimidazole (**23**). We examined the MAO substrate properties of **64** by the same techniques described above. The HPLC-UV/Vis-DA tracings are reported below.

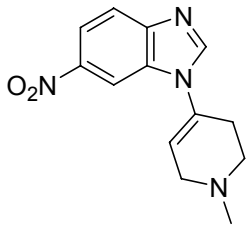


**64**

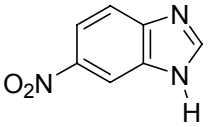


**23**

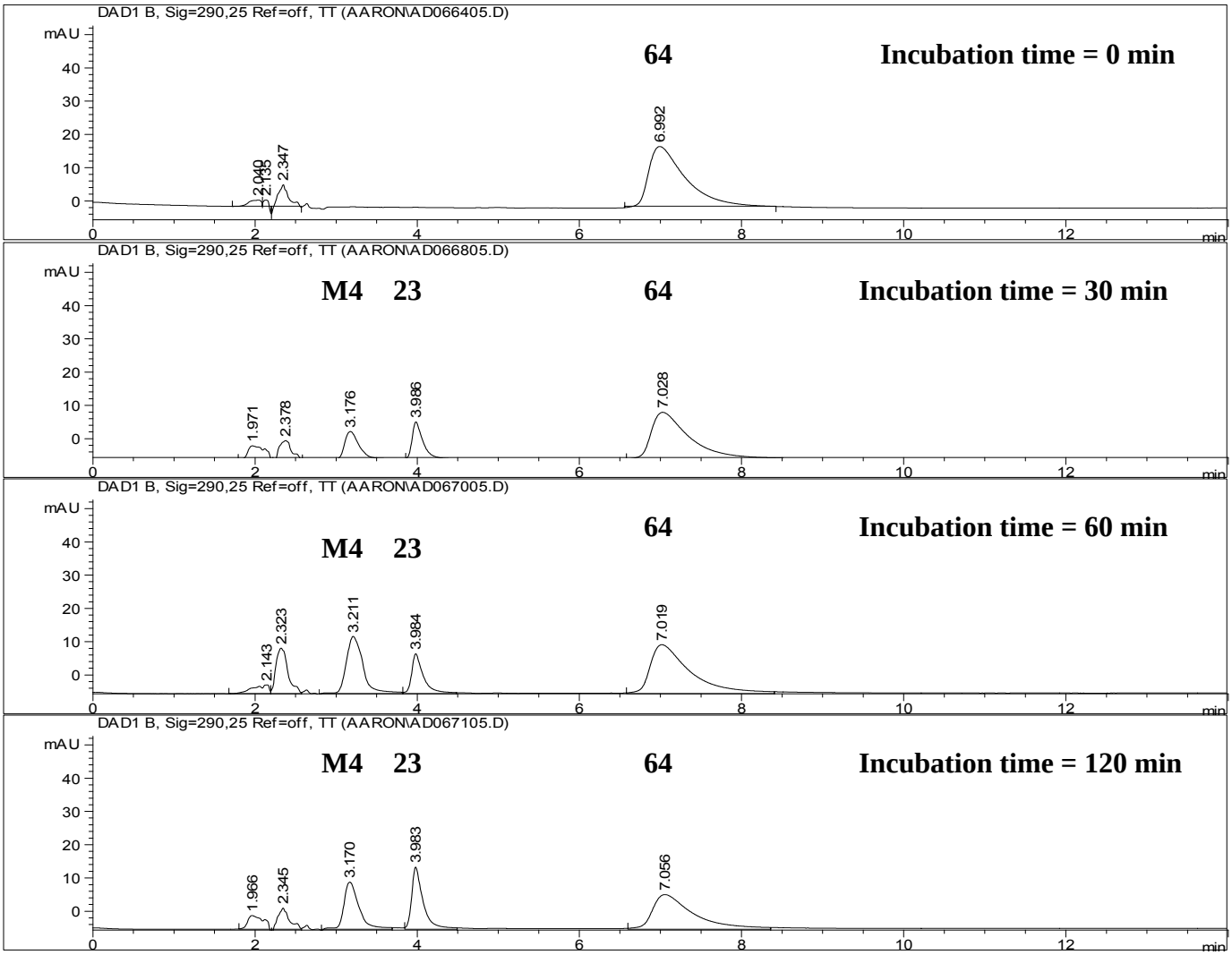


**Figure 19. HPLC analysis of supernatants from incubation mixtures of 64 with MAO-B.**

**Figure 19** shows the fate of **64** upon MAO-B activation. A similar experiment with the A form of the enzyme gave analogous results. As expected, the peak at ~ 7 minutes corresponding to substrate **64**, decreased with time. Furthermore, two metabolite peaks increased with time. The peak with a retention time of 4 minutes was tentatively identified as 6-nitrobenzimidazole (**23**). This was confirmed by a comparison of the UV spectra (**Figure 20**) of the standard 6-nitrobenzimidazole (purchased from Aldrich) and that formed during the enzyme assay.

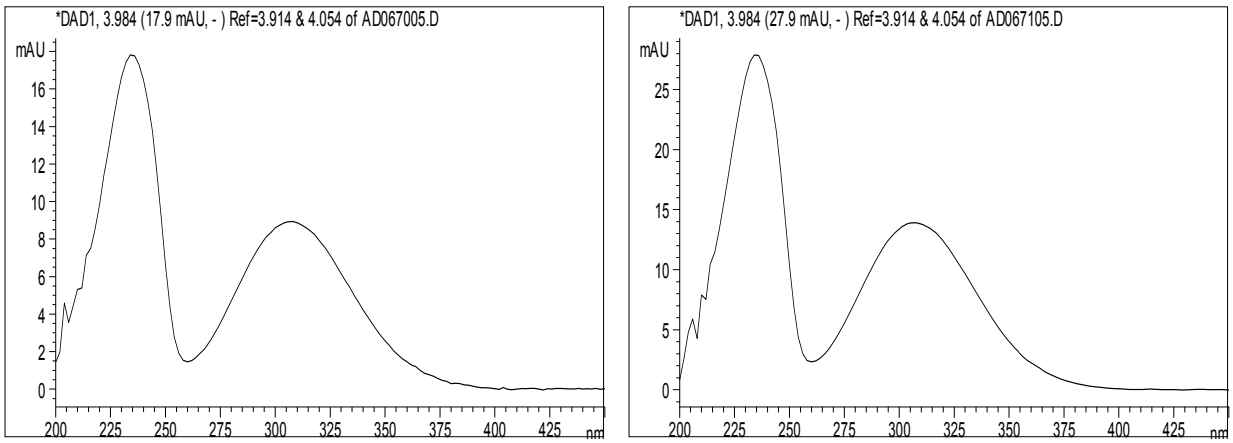


**Figure 20. UV spectra of 6-nitrobenzimidazole (23). Standard (left).**

The structure of **M4**, the other metabolite formed in this incubation mixture, was not obvious. The retention time (3.2 minutes) of the metabolite corresponds to that of the 1-methyl-4-(6-nitrobenzimidazol-1-yl)pyridinium species **70**. However, comparison of the UV spectra (**Figure 21**) did not confirm this assignment.

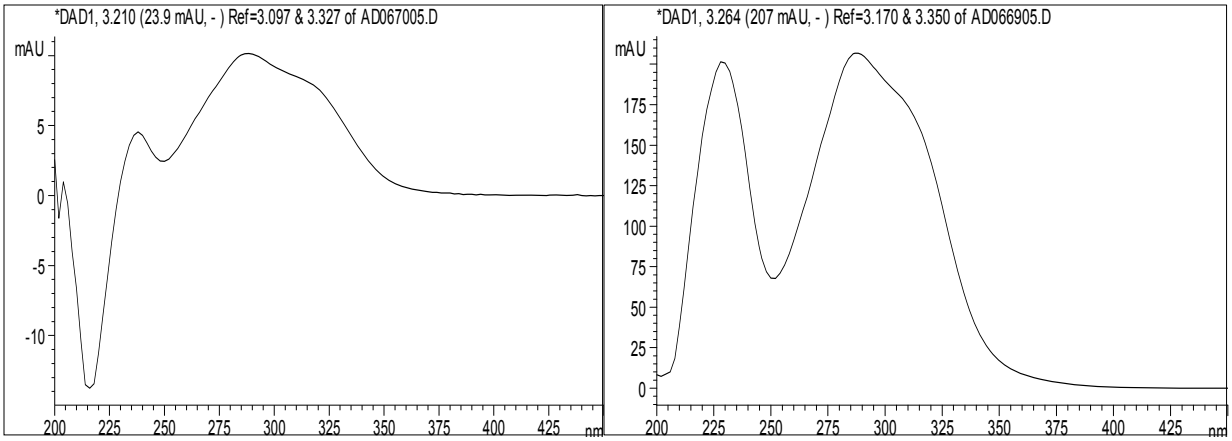


**Figure 21. UV spectra of M4 (left) and 70 (right).**

Another possible assignment for **M4** would be the aminoenone **27** that would form upon hydrolysis of dihydropyridinium species **66** (see Scheme 17). Compound **27** was not commercially available and had to be synthesized. This was done according to literature.[51] The HPLC data for the synthetic aminoenone **27** and **M4**, however, were not the same. Although the synthetic aminoenone **27** had a retention time of ~ 3.2 minutes (similar to **M4**), the UV spectrum was different from that of **M4** (**Figure 21**). Finally, it was proposed that the unidentified peak at 3.2 minutes corresponded to a mixture of the previously mentioned metabolites (**70** and **27**). To confirm this theory, the supernatants from the enzyme assay were examined using LC-MS. The results from this analysis are reported below (**Figure 22** and **Figure 23**).

[51] Yasumitsu T., Masaru K., Takehiko M., and Masanao T. (1972). Partial reduction of 4-pyridones with $LiAlH(OC_2H_5)_3$: Syntheses of 2, 3-dihydro-4-pyridones. *Chemistry and Industry*. 19 February 1972, 168-169.

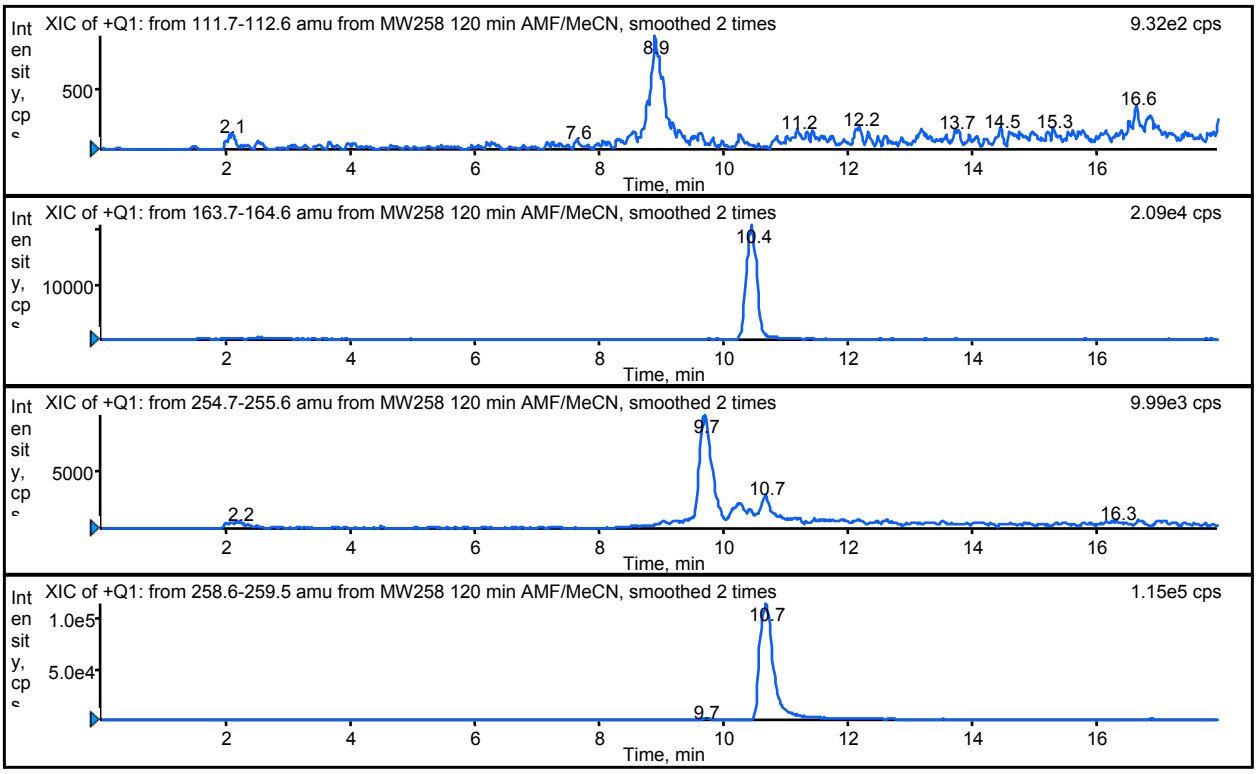


**Figure 22. Extracted Ion Chromatograms (XIC) from the incubation mixture with substrate 64 and MAO-B for 120 minutes.**

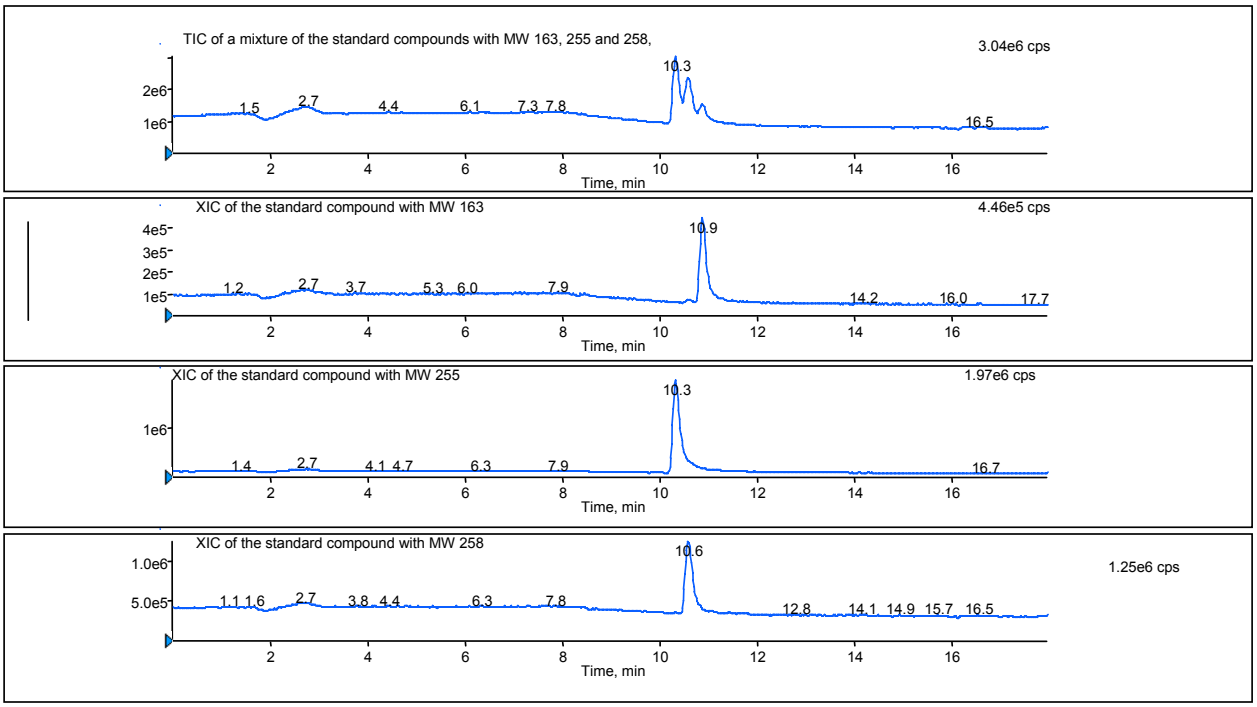


**Figure 23. TIC and SIM Chromatograms Obtained from a Mixture of the Standard Compounds 23, 64, and 70**

The comparison of **Figure 22** with **Figure 23** provided evidence for the formation of two out of three suspected metabolites from the MAO-B bioactivation of **64.** One of these was the previously identified 6-nitrobenzimidazole (**23**), which has a m/z of 164. The other metabolite identified from this comparison was **70** (m/z = 255). This was verified by means of a comparison of the synthetic standards with the supernatant from the enzyme assay. The bioassay was conducted and the bioactivated metabolites had generally the same retention times (the differences in retention times are likely due to the fact that the standards were run at a different time and the column had aged. The conditions of the mass spectrometer were also different.). The aminoenone **27** (m/z = 112) also appears to have formed during the bioactivation as there is a peak in **Figure 22** with a m/z equal to 112. This suggests that the peak (labeled **M4**) at 3.2 minutes in **Figure 19** represents a mixture of compounds that are identified as **70** and **27** by LC/MS. It should be noted that the parent ions of the uncharged molecules are $MH^+$, whereas the parent ion of the pyridinium (**70**) being a charged molecule is $M^+$.

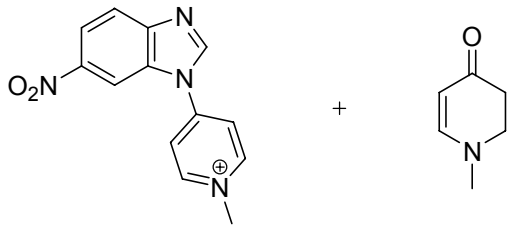

**70** **27**

### 3.2.5 Investigation of the 6-NBI prodrug kinetics with MAO-B

After discovering that the 6-NBI prodrug **64** releases the MAO-B inhibitor 6-NBI (**23**) upon bioactivation, we determined the enzyme kinetics of this reaction. We examined the enzyme kinetics as a function of the concentration of substrate available to the enzyme. The study design paralleled that reported above. The initial velocity (Vi) was

determined during the early phases of the reaction when the substrate concentration was in large excess. These values were determined by taking the slopes of the linear series as shown in **Figure 24**.

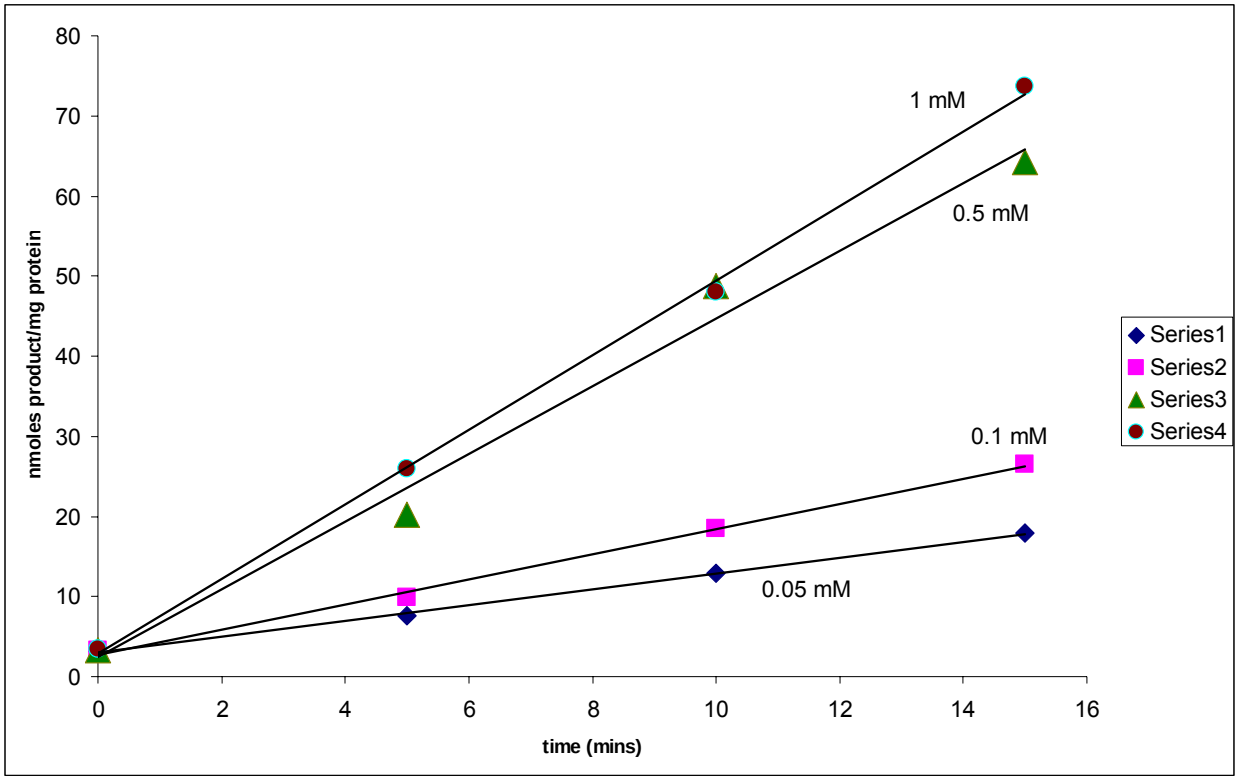


**Figure 24. Determination of $V_i$ at different concentrations.**

Plotting $V_i$ vs. [**S**] (**Figure 25**) provided a graph that gives the enzyme kinetic values $K_m$ and $V_{max}$. As substrate concentration increases, the increase in $V_i$ level off until $V_{max}$ is reached and the rate of product formation is constant with time.

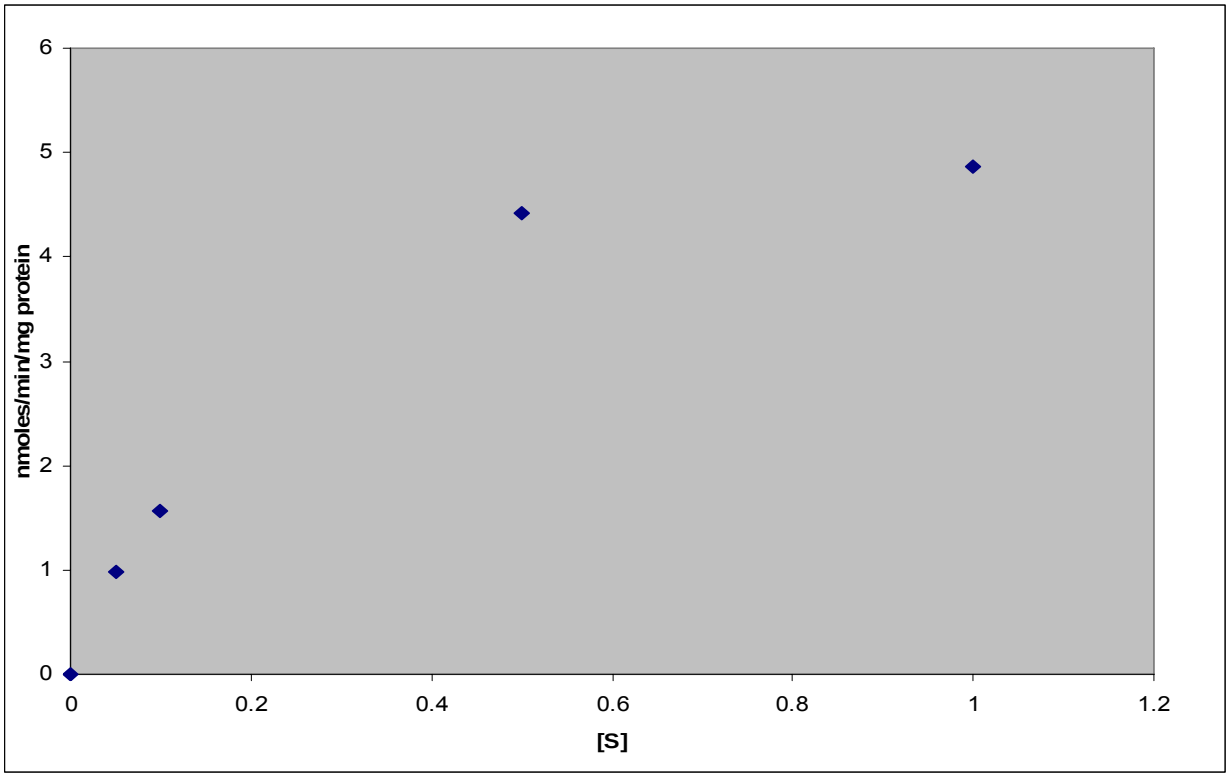


**Figure 25. Determination of $K_m$ and $V_{max}$ of 64 with MAO-B**

By examining **Figure 25**, $V_{max}$ and $K_m$ can be approximated; however, as mentioned earlier, plotting the reciprocals of the same data points yields a linear plot (LIneweaver-Burke) that gives the values with simple algebra (**Figure 26**).

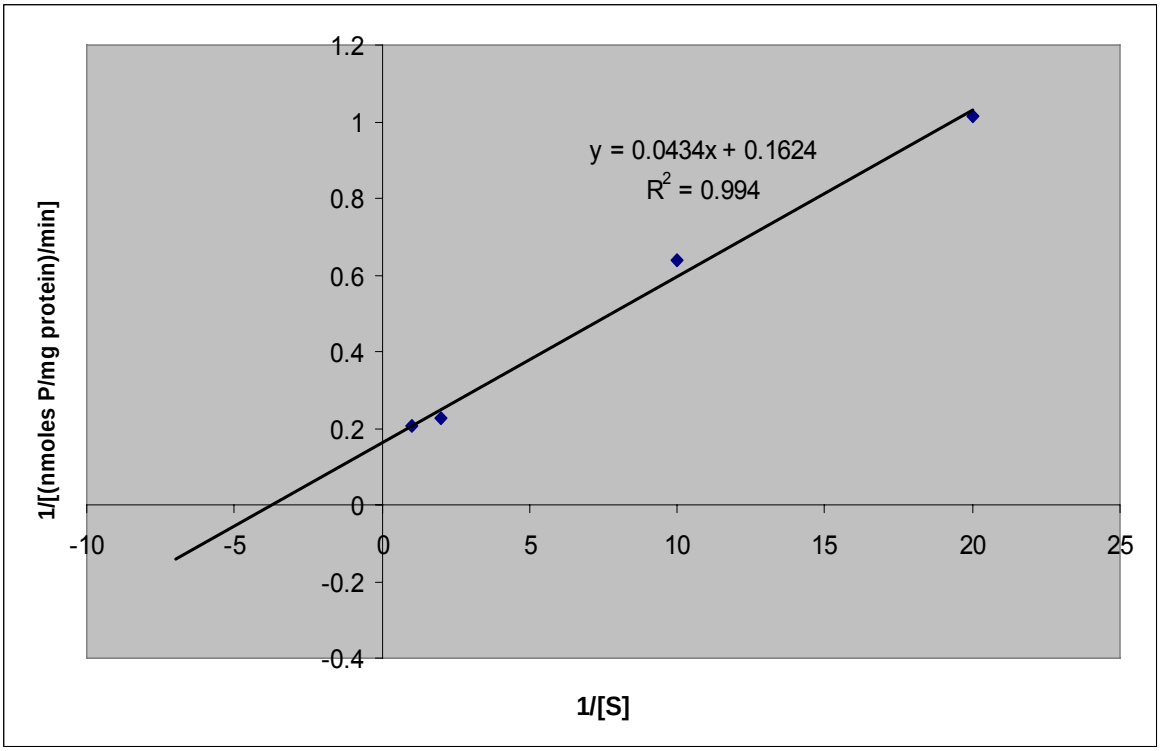


**Figure 26. Lineweaver-Burk plot of Figure 23.**

From **Figure 25**, $V_{max}$ was determined by the point where the line crosses the y axis at x = 0 ($1/V_{max}$). The $V_{max}$ for the 6-NBI prodrug was estimated to be 6.16 ± 4.3 nmol/mg protein/minute. $K_m$ equals $V_{max}$ times the slope of the line. This can easily be determined from the intercept on the X axis. The $K_m$ for the 6-NBI prodrug is equal to 0.267 ± 0.18 mM.

### 3.2.6 *In Vivo* Investigation of the 6-NBI prodrug 64.

This study was undertaken with the help of Mrs Kay Castagnoli who performed injections and all dissections, Dr. Philippe Bissel (injections) and Ms. Rachel Piggott (who helped with the HPLC-EC analysis). Based on what was observed in each of the above *in vitro* studies, we concluded that the only worthwhile *in vivo* study to pursue

would be with the 6-NBI prodrug **64**. As reviewed in **Section 2.2**, we were hopeful that the release of an MAO-B inhibitor following bioactivation might protect against the neurotoxicity of MPTP (**2**).

The neuroprotection studies were undertaken in the C57BL/6 MPTP Parkinsonian model. In this model, MPTP is bioactivated in the brain by MAO-B to form the dihydropyridinium and the $MPP^+$ as discussed in **Section 1.2**. The toxicity of $MPP^+$ leads to dopamine depletion in the nigrostriatum of the mouse. Pretreatment of the animal prior to administration of the neurotoxin leads to protection of the dopaminergic neurons and thus protection against loss of dopamine in the striatum. In these studies, the DA levels of the striata will be measured using HPLC with electrochemical detection and compared in animals treated with MPTP to dopamine levels in the striata of animals pretreated with the putative prodrug **64** prior to MPTP administration.

Before the neuroprotective study could be conducted, the acute toxicity of prodrug **64** had to be evaluated in the target animal, the C57C/BL6 mouse. The dual toxicity of **64** along with MPTP (**2**) was also evaluated. The first dose of **64** (107 mg/kg) given was the same molar dose as **1** (7-NI) that had been given in a previous study and had provided neuroprotection.[52] This dose of **64** proved to be fatal and the dose was reduced to 20% (21.4 mg/kg) of this initial concentration for the subsequent injection. This dose was also toxic (the two mice given this dose were clearly experiencing toxic effects) although this did not lead to death. The next toxicity test was performed using both the prodrug (**64**)

---

[52] Castagnoli, K., Palmer, S. and Castagnoli, N. Jr. (1999) Neuroprotection by (*R*)-Deprenyl and 7-Nitroindazole in the MPTP C57BL/6 mouse model of neurotoxicity. *Neurobiology*. **7**, (2) 135-149.

and MPTP (**2**). Since the 21.4 mg/kg dose of **64** showed toxicity, it was decided to examine the dual toxicity (**64** and **2**) at a dose of 10.7 mg/kg of **64** and 35 mg/kg of MPTP (**2**), a dose of MPTP known to lead to striatal dopamine depletion. Unfortunately, most of the animals died as a result of this combination.

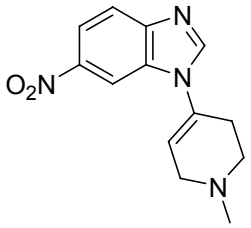


**64**

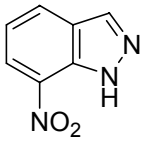


**1**

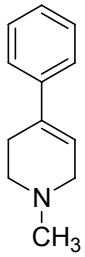


**2**

Finally, 8.025 mg/kg (7.5 % of original dose) of **64** and 30 mg/kg of MPTP (**2**) led to no obvious signs of toxicity and the neuroprotective study of interest was pursued using this dosage regimen.

After finding the acceptable dose of both prodrug **64** (8.025 mg/kg) and MPTP (30 mg/kg) (**2**), the neuroprotective experiment was designed. It was decided to use 4 groups of animals for the study. Based on a previous study,[52] each group received two injections administered 15 minutes apart. The control group received only i.p. saline. The second group, the MPTP-treated group, was injected ip with saline first followed by MPTP. The third group was the prodrug (**64**)/MPTP-treated group. This group received **64** first followed by MPTP (**2**). This groups' dopamine levels could be compared to the previously mention group (MPTP only) to determine if any protection occurred. The final group of the study received an injection of prodrug **64** only. This was done to determine

if any effects on dopamine levels occurred as a result of the prodrug (**64**). On day 7 following the injections (all injections were performed by Kay Castagnoli and Philippe Bissel), the mice were sacrificed. The striata were dissected (dissections by Kay Castagnoli) and analyzed for dopamine levels using HPLC with electrochemical detection (HPLC-EC work done with help from Rachel Piggott).

The HPLC-EC assay was conducted to determine the striatal dopamine levels of the four groups used in the study. Dopamine is one of the most studied electrochemically active structures and its relative concentration can be determined from the corresponding current generated during the oxidation reaction (**Scheme 20**).[53]

**Scheme 20:** HPLC-ED oxidation of dopamine

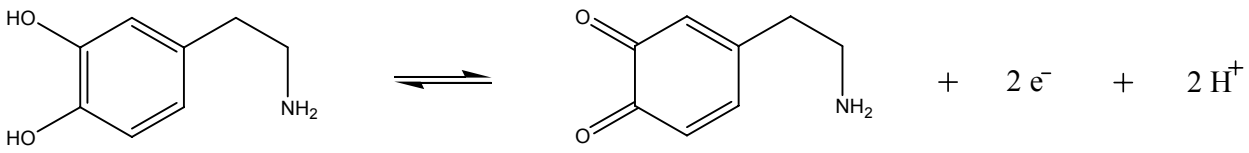


**19** **71**

Oxidation occurs when a species loses electrons as seen with dopamine (**19**) in **Scheme 20**. The electron transfer generates an electric current on the electrode surface of the cell. Faraday's Law that states "the amount of substance consumed or produced at one of the electrodes in an electrolytic cell is directly proportional to the amount of electricity that passes through the cell." If different concentrations are present, different

[53] Flanagan, R.J., Perrett, D., and Whelpton, R. (2005) Electrochemical Detection in HPLC – Analysis of drugs and poisons. *RSC Chromatography Monographs*. 6-20.

electrical currents should be transported and different currents would be observed. We have analyzed the striatal extracts from the four groups of the study designed above following this approach using an established assay[52] and the results from the analysis are below in **Figure 25**. The results are based on the peak height ratios of DA to dihydroxybenzylamine (DHBA), the internal standard.

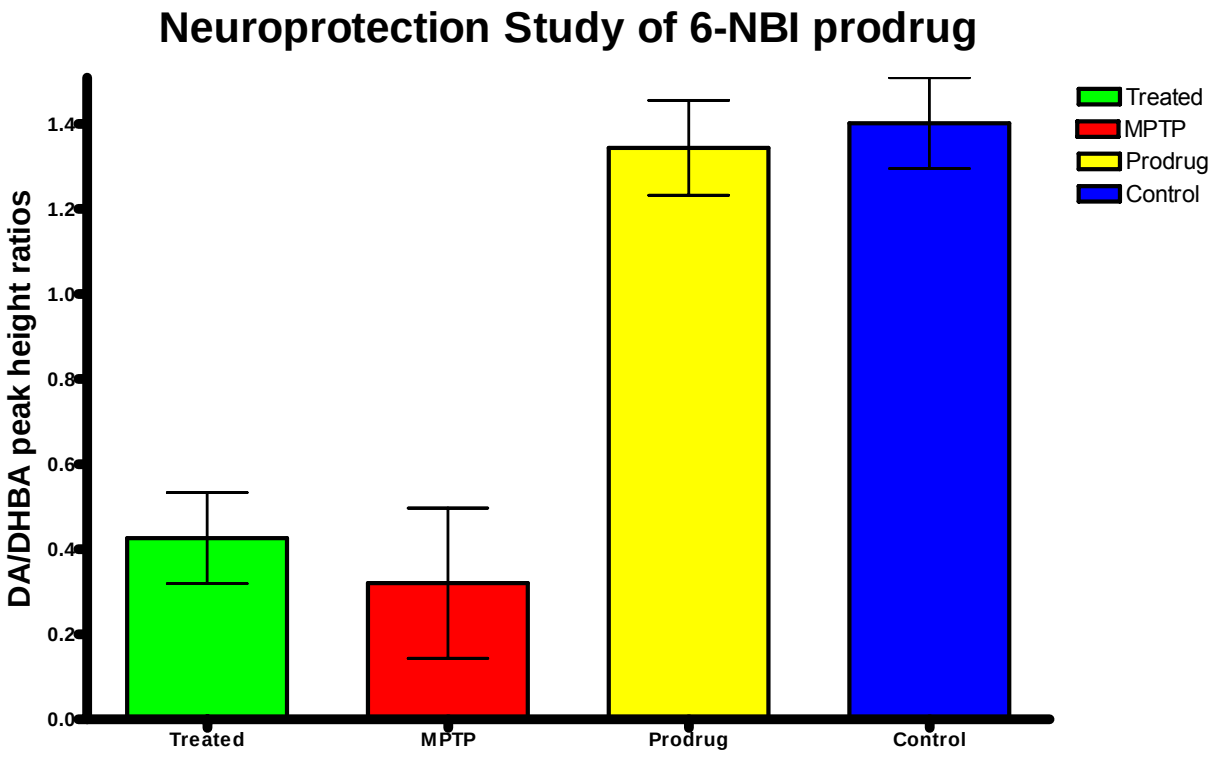


**Figure 27. Results of Neuroprotective study using prodrug 64**

The results (peak height ratio of DA/DHBA) establish that, under these experimental conditions, compound **64** does not protect against the toxicity of MPTP. The statistical analysis of the data using Prism software confirms that the minor difference in dopamine levels between the MPTP only and the MPTP plus **64** is not statistically

significant. Therefore we conclude that prodrug **64** is not a neuroprotective agent against MPTP toxicity with the dose administered in the present study.

## 4.0 Conclusions

According to the "Prodrug" concept under consideration, in which a tetrahydropyridinyl moiety has been attached to several known inhibitors (**16, 17,** and **23**) of MAO-B, we have discovered one compound out of this series that is bioactivated by MAO-B to release an inhibitor of the enzyme. The compound found was the benzimidazole prodrug **64** and the bioactivation was discovered with the HPLC assay discussed above (**3.2.4**). The purpose of identifying and synthesizing such a compound(s) was to overcome an obstacle encountered in a previous *in vivo* study.[50] This obstacle seen earlier was the insolubility of the MAO-B inhibitor 7-NI (**1**). Furthermore, the prodrug **1** of 7-NI was unsuccessful in releasing the inhibitor upon bioactivation with MAO-B.[1]

While we have discovered an interesting substrate (**64**) for MAO-B that releases the parent inhibitor during *in vitro ex*periments**,** the compound did not meet anticipations in the MPTP mouse model. Based on the results shown in **Figure 27**, we conclude that **64** did not protect against the neurotoxicity of MPTP in the experimental paradigm utilized. The reason(s) for this are not immediately obvious. However, several theories can be postulated. One explanation is related to the toxicity of the prodrug. We were unable to administer a dose that, based on previous results, might be required to protect against MPTP's toxicity,[50] since this dose of **64** proved to be lethal. Brain levels of **64** were not measured and thus it is not known if we achieved brain concentration of **64** which were greater than $K_i$. It is possible that systemic metabolism prevented the prodrug from reaching adequate concentrations in the brain to be neuroprotective. As previously discussed, MAO is present in other organs of the body and it may be that the substrate

(**64**) was metabolized in peripheral organs that prevented it reaching the required brain concentrations. Furthermore, the prodrug **64** is not selective for either form of MAO; that is **64** is a substrate for MAO-A and MAO-B. If the substrate reacts primarily with MAO-A *in vivo*, increased serotonin levels would be expected while no change would be expected in the dopamine levels compared to animals not pre-treated with **64**.

A further outcome of the current study was the synthesis of the pyridinium intermediates **62** and **63** as precursors to the desired 2*H*-prodrugs **30** and **32**. These compounds also were needed in order to characterize the metabolites generated from these regioisomeric prodrugs of the nitroindazole systems (**16** and **17**) under consideration. Syntheses of these isomers have been attempted in the past but the desired products were not obtained. We have found a procedure that was successful for their synthesis. It involved performing the reaction in the absence of both base and solvent. The two starting materials (**16** and **58**, see **Section 3.1.1**), which were solids, were added together to give a neat reaction.

Since a pair of regioisomers could be obtained with the indazolyl system, confirmation of the regiochemical outcomes of these reactions was required. This was done using 2D-NOESY NMR spectroscopy to identify the through-space interactions of the protons relevant to the location of substitution. The two pyridiniums species **62** and **63** were identified unambiguously. However, C, H, and N analysis proved that the products were not the expected iodide salts but rather the triiodide salts **67** and **68**. Subsequent reduction using $NABH_4$ ultimately led to the desired 2*H*-prodrugs **30** and **32**.

Finally, the newly synthesized 2*H*-prodrugs were tested for MAO activity. It was determined that these regioisomers had no MAO-B activity (see **Section 3.2.2**) and thus could not provide the necessary neuroprotection in the MPTP PD mouse model we were seeking in our prodrugs. Interestingly, the 2*H*-isomers also are substrates for MAO-A. The significance of the mixed-substrate properties of these compounds needs further evaluation.

## 5.0 Experimental

### 5.1 Chemistry

**1-Methyl-4-chloropyridinium iodide (58)**. This compound was prepared according to the literature.[54] The 4-chloropyridine hydrochloride salt (12.06 g, 80.4 mmol) was converted into the free base by dissolving it in water and treating it with (sat.) $K_2CO_3$ until the pH was 9. The free base was then extracted with $CH_2Cl_2$. The $CH_2Cl_2$ was dried with $NaSO_4$ and the solvent was evaporated. Methyl iodide (45.6 g, 322 mmol) was added dropwise at 0°C over a period of 15 minutes. It was stirred at 0°C for 2 hrs. The reaction was left overnight at room temperature. The product was filtered and recrystallized from MeOH/Ether to give 14.32 g (69.8 % yield) of a yellow solid; mp 160-161.6 °C Known compound (161-163 °C). $H^1$-NMR (DMSO-$d_6$, 400 MHz): δ 9.0 (d, 2H, J = 6.8 Hz), δ 8.4 (d, 2H, J = 6.8 Hz), δ 4.3 (s, 3H).

**1-Methyl-4-(5-nitroindazol-1-yl)pyridinium iodide (61).**This compound was prepared according to the literature.[1] To a solution of 5-nitroindazole (**16**) (1.32 g, 8.08 mmol) in 25 mL of N,N-dimethylformamide, 1-methyl-4-chloropyridinium iodide (1.90g, 8.08 mmol) was added. To this solution, 2,2,6,6-tetramethylpiperidine (1.36 mL, 8.08 mmol) was added. The reaction was stirred for 2 hours at room temperature. It was recrystallized from methanol/ether (50:50) to give 2.0 g (66%) of a yellow solid; mp 280-281 °C Known compound (280-281 °C). $^1$H NMR (DMSO-$d_6$, 400 MHz):

**1-Methyl-4-(6-nitroindazol-1-yl)pyridinium iodide (62)**. This compound was prepared according to the literature.[1] To a solution of 6-nitroindazole (**17**) (1.32 g, 8.08 mmol) in 25 mL of N,N-dimethylformamide, 1-methyl-4-chloropyridinium iodide (1.90g,

[54] Sprague, R. H., Brooker, L. G. S. (1937) Studies in the cyanine dye series. IX. 4, 4′-pyridocyanines and 4-pyrido-4′-cyanines. *J. Am. Chem. Soc.* **59**, 2697-2699.

8.08 mmol) was added. To this solution, 2,2,6,6-tetramethylpiperidine (1.36 mL, 8.08 mmol) was added. The reaction was stirred for 2 hours at room temperature. After this, the reaction was filtered to give 2.76 g of crude product. It was recrystallized from methanol/water (50:50) to give 1.95 g (63.2%) of a yellow solid; mp 283-284.5 °C Known compound (283-284°C).[1] $^1$H NMR (DMSO-$d_6$, 400 MHz): δ 9.0 (m, 4H), δ 8.6 (d, 2H, J = 7.2 Hz), δ 8.3 (m, 2H) δ 4.4 (s, 3H).

**1-Methyl-4-(5-nitroindazol-2-yl)pyridinium triiodide (67).** 5-Nitroindazole (**16**) (4.45 g, 27.3 mmol) and 1-Methyl-4-chloropyridinium iodide (3.21 g, 13.7 mmol) were placed in a flask under nitrogen and heated until the mixture melted at 150 °C. The flask was allowed to cool to room temperature. The solid that remained was washed with 200 mL of ether. The obtained solid was recrystillized from acetone to give 850 mg (9.79 %) of product; mp = 232-234 °C; $^1$H NMR (DMSO-$d_6$, 400 MHz): δ 9.93 (d, 1H, J = 0.8 Hz), δ 9.2 (d, 2H, J = 7.2 Hz), δ 9.0 (dd, 1H, $J_1$ = 1.2 Hz, $J_2$ = 0.4 Hz), δ 8.9 (d, 1H, J = 3.6 Hz), δ 8.2 (dd, 1H, $J_1$ = 7.6 Hz, $J_2$ = 2 Hz), δ 8.0 (d, 1H, J = 1.6 Hz), δ 4.4 (s, 3H). $^{13}$C NMR (DMSO-$d_6$, 100 MHz) δ 151, 150, 148, 144, 130, 123, 121.9, 121.8, 119, 117, 47. Anal. Calcd for $C_{13}H_{11}N_4O_2I_3$: C, 24.55; H, 1.74; N, 8.81; I, 59.86. Found: C, 24.72; H, 1.75; N, 8.78; I, 59.65.

**1-Methyl-4-(6-nitroindazol-2-yl)pyridinium triiodide (68).** 6-Nitroindazole (**17**) (6.58 g, 40.4 mmol) and 1-methyl-4-chloropyridinium iodide (1.90 g, 8.08 mmol) were placed in a flask under nitrogen and heated until they were both melted. It was heated to 160°C and stirred for 5 minutes. The solid was washed with ether several times and filtered. It was recrystillized with MeOH to give 1.47 g (28.7% yield); mp = 218-220°C; $^1$H NMR (DMSO-$d_6$, 400 MHz): δ 9.9 (d, 1H, J = 1.2 Hz), δ 9.3 (d, 2H, J = 7.2 Hz), δ 8.9

(d, 2H, J = 7.2 Hz), δ 8.8 (t, 1H, $J_1$ = 1.2 Hz, $J_2$ = 0.8 Hz), δ 8.2 (dd, 1H, $J_1$ = 8.4 Hz, $J_2$ = 0.8 Hz), δ 7.9 (dd, 1H, $J_1$= 7.2 Hz, $J_2$ = 2 Hz), δ 4.4 (s, 3H). $^{13}$C NMR (DMSO-$d_6$, 100 MHz) δ 150, 149, 148.88, 148.38, 127, 125, 124, 117, 116, 48. Anal. Calcd for $C_{13}H_{11}N_4O_2I_3$: C, 24.55; H, 1.74; N, 8.81; I, 59.86. Found: C, 24.81; H, 1.70; H, 8.53; I, 59.60.

**1-Methyl-4-(6-nitrobenzimidazolyl) pyridinium iodide (70)**.

5-nitrobenzimidazole (1.09 g, 6.68 mmol) and 1-methyl-4-chloropyridinium iodide (1.57 g, 6.68 mmol) were dissolved in 30 mL DMF. This mixture was heated to 70 °C and stirred for 4 hours. The reaction was then cooled to room temperature and filtered. 2.06 g of a yellow solid was obtained.$^1$H NMR revealed the formation of the two possible regioisomers. Recrystallization with MeOH provided a solid (1.23 g) that was primarily one product with trace amounts of the opposite regioisomer. mp = 242-244 °C; $^1$H NMR (DMSO-$d_6$, 400 MHz): δ 9.3 (s, 1H), δ 9.22 (d, J = 7.2 Hz, 2H), δ 8.82 (d, J = 2.4 Hz, 1H), δ 8.66 (d, J = 7.2 Hz, 2H) , δ 8.35 (dd, $J_1$ = 2.4 Hz, $J_2$ = 9.2 Hz, 1H), δ 8.1 (d, J = 8.8 Hz, 1H), δ 4.42 (s, 3H).

**Oxalate salt of 1-methyl-4-(5-nitroindazol-1-yl)-1,2,3,6-tetrahydropyridine (29)**. To a suspension of 1-methyl-4-(5-nitroindazol-1-yl) pyridinium iodide (2.00g, 5.24 mmol) under nitrogen in methanol (52 mL) was added sodium borohydride (0.794 g, 21 mmol) over a period of 15 minutes. After 1 hour, the methanol was evaporated. The solid obtained was extracted between a saturated NaCl solution and $CH_2Cl_2$. The organic layer was dried with $Na_2SO_4$ and the solvent was evaporated. 1.11 g (82 %) of the free base was obtained. It was treated with 1.2 equivalents of oxalic acid (0.464 g, 5.16 mmol) to give 1.49 g of the oxalate salt. This was recystallized to

give 1 g (67 %) of product: mp = 201-203°C; $^1$H NMR (DMSO-$d_6$, 400 MHz): δ 8.9 (d, 1H, J = 2 Hz), δ 8.6 (s, 1H), δ 8.30-8.33 (dd, 1H, $J_1$ = 2 Hz, $J_2$ = 7.2 Hz), δ 7.99-8.02 (d, 1H, J = 9.2 Hz), δ 6.26 (s, 1H), δ 3.79 (unresolved multiplet, 2H), δ 3.3 (unresolved multiplet, 2H), δ 2.9 (unresolved multiplet, 2H), δ 2.79 (s, 3H). Anal. Calcd. for $C_{15}H_{16}N_4O_6$ with 0.5 mol $H_2O$: C, 50.42; H, 4.80; N, 15.68. Found: C, 50.55; H, 4.82; N, 15.62.

**Oxalate salt of 1-methyl-4-(6-nitroindazol-1-yl)-1,2,3,6-tetrahydropyridine (31)**. To a suspension of 1-methyl-4-(6-nitroindazol-1-yl)pyryidinium iodide (2.00 g, 5.24 mmol) under nitrogen in methanol (50 mL) was added sodium borohydride (0.794 g, 21 mmol) in portions over a period of 15 minutes. After 2 hours, the methanol was evaporated. The solid obtained was extracted between a saturated NaCl solution and $CH_2Cl_2$.The organic layer was dried with $Na_2SO_4$ and the solvent was evaporated. 1.04 g (77 %) of the free base was obtained. It was treated with 1.2 equivalents of oxalic acid (0.435 g, 4.84 mmol) to give 1.273 g (90 %) of the oxalate salt: mp = 215-216ºC; $^1$H NMR (DMSO-$d_6$, 400 MHz) : δ 8.64 (s, 1H), δ 8.55 (s, 1H), δ 8.07-8.14 (m, 2H), δ 6.32 (s, 1H), δ 3.85 (s, 2H), δ 3.36-3.39 (unresolved multiplet, 2H), δ 3.0 (unresolved multiplet, 2H), δ 2.83 (s, 3H). Anal. Calcd. for $C_{15}H_{16}N_4O_6$ with 1 mol $H_2O$: C, 49.18; H, 4.95; N, 15.29. Found: C, 49.39; H, 4.94; N, 15.47.

**Oxalate salt of 1-methyl-4-(5-nitroindazol-2-yl)-1,2,3,6-tetrahydropyridine (30)**. Sodium borohydride (0.186 g, 4.91 mmol) was added in portions to a suspension of **59** (0.780 g, 1.23 mmol) in 15 mL of methanol over a 5 minute period. After 2 hours, the methanol was evaporated. The solid was extracted between $CH_2Cl_2$ and (sat.) NaCl. The $CH_2Cl_2$ layer was dried with $NaSO_4$. The solid

obtained (0.270 g, 85.2% yield) was converted to the oxalate salt by treating it with 1.2 equivalents of oxalic acid in ether: mp = 204 – 205 °C; $^{1}$H NMR (DMSO-$d_6$, 400 MHz): δ 9.06 (s, 1H), δ 8.81 (d, 1H, 2 Hz), δ 8.0 (dd, 1H, $J_1$ = 2 Hz, $J_2$ = 9.2 Hz), δ 7.78 (d, 1H, J = 9.2 Hz), δ 6.67 (s 1H), δ 3.72 (unresolved multiplet, 2H), δ 3.27 (unresolved multiplet, 2H), δ 3.02 (unresolved multiplet, 2H), δ 2.71 (s, 3H). $^{13}$C NMR (DMSO-$d_6$, 100 MHz) δ 161, 143, 141, 137, 126, 124, 123, 119.5, 119, 113.6, 54, 49, 46, 27.

**Oxalate salt of 1-methyl-4-(6-nitroindazol-2-yl)-1,2,3,6-tetrahydropyridine (32)**. Sodium Borohydride (0.97 g, 25 mmol) was added in portions to a suspension of **60** (4.05 g, 6.37 mmol) in 35 mL of methanol over a 15 minute period. After 2 hours, the methanol was evaporated. The solid was extracted between $CH_2Cl_2$ and (sat.) NaCl. The $CH_2Cl_2$ layer was dried with $NaSO_4$. The solid that was obtained was dissolved in methanol and treated with 1.2 equivalents of oxalic acid in ether to give 0.74 g (33 %) of the oxalate salt: mp = 177-179 °C; $^{1}$H NMR (DMSO-$d_6$, 400 MHz) δ 9.00-9.01 (m, 1H), δ 8.67-8.68 (m, 1H), δ 8.00-8.03 (dd, 1H, $J_1$ = 8.8 Hz, $J_2$ = 0.4 Hz), δ 7.84-7.87 (dd, 1H, $J_1$ = 7.2 Hz, $J_2$ = 2.0 Hz), δ 6.72-6.74 (m, 1H), δ 3.712 (unresolved multiplet, 2H), δ 3.25-3.28 (t, 2H, $J_{1,2}$ = 5.6 Hz), δ 3.0 (unresolved multiplet, 2H), δ 2.73 (s, 3H). $^{13}$C NMR (DMSO-$d_6$, 100 MHz) δ 164, 147, 146, 134, 124, 123.4, 123.2, 116, 115, 113, 51, 49, 42, 23.

**Oxalate salt of 1-methyl-4-(6-nitrobenzimidazolyl)-1,2,3,6-tetrahydropyridine (64).** Sodium borohydride (0.48 g, 13 mmol) was added in portions to a suspension of **70** (1.20 g, 3.14 mmol) in mL of methanol over a 10 minute time period. After 3 hours, the methanol was evaporated. The solid was extracted between $CH_2Cl_2$ and (sat.) NaCl. The $CH_2Cl_2$ layer was dried with $NaSO_4$. The solid obtained

was converted to the oxalate salt (0.82 g, 76% yield) by treating it with 1.2 equivalents of oxalic acid in ether: 194-196 °C; $^{1}$H NMR (DMSO-$d_6$, 100 MHz): δ 8.77 (s, 1H), δ 8.52 (d, 1H, 2 Hz), δ 8.14-8.16 (dd, 1H, $J_1$ = 8.4 Hz, $J_2$ = 2 Hz), δ 7.89-7.91 (d, 1H, 9.2 Hz), δ 6.23-6.25 (unresolved multiplet, 1H), δ 3.77-3.78 (d, 2H, 2.4 Hz), δ 3.31-3.34 (t, 2H, 6 Hz), δ 2.90-2.91 (d, 2H, 1.6), δ 2.774 (s, 3H). $^{13}$C NMR (DMSO-$d_6$, 400 MHz) δ 164, 148, 147, 143, 132, 130, 120, 118, 117, 108, 51, 50, 42, 26. Anal. Calcd. for $C_{15}H_{16}N_4O_6$: C, 51.72; H, 4.63; N, 16.09. Found: C, 51.59; H, 4.76; N, 16.20.

## 5.2 Biology

### a. MAO preliminary experiments

Preliminary experiments[1] were performed on the test compounds to determine if they were substrates for MAO-A/B. This was done following an assay procedure done previously. However, it was modified slightly to obtain a better signal:noise ratio on the spectra. The stock solution of the test compound (2 mM) was prepared in pH 7.4 0.1 M sodium phosphate buffer. Enzyme (25 µL, 6 mg protein/ml) was added to incubation mixtures (pre-equilibrated at 37 °C) consisting of pH 7.4 0.1 M phosphate buffer (435 µL) and the test compound (40 µL) to yield a final concentration of 160 µM. The final volume of the incubation mixtures was 500 µL and the final protein concentration was 0.3 mg/ml. These mixtures were incubated with gentile agitation in a water bath at 37 °C for 0, 30, 60, 120 minutes. Acetonitrile (500 µL) was added and the resulting mixture was vortex agitated. The denatured protein was sedimented by centrifugation at 10,000 g for 6 minutes. The supernatants (50 µL) were applied to HPLC-UV/Vis-DA.

**b. MAO Kinetic analysis**

A stock solution (4 mM) of substrate was prepared in pH 7.4 0.1 M phosphate buffer. Enzyme (50 µL, 6 mg/mL) was added to incubation mixtures (pre-equilibrated at 37 °C) consisting of pH 7.4 0.1 M phosphate buffer (443.75 µL, 437.5 µL, 387.5 µL, and 325 µL) and test compound (6.25 µL, 12.5 µL, 62.5 µL, and 125 µL) to yield the final concentrations of 0.05, 0.1, 0.5, and 1 mM. The final volume of the incubation mixtures was 0.5 mL and the final protein concentration was 0.3 mg/mL. These mixtures were incubated with gentle agitation in a water bath at 37 °C from 0-60 mins. Every 5 minutes, acetonitrile was added and the resulting mixture was vortex agitated. The denatured protein was sedimented by centrifugation at 10,000 g for 6 minutes. The supernatants (50 µL) were applied to HPLC-UV-DA. Initial rates of oxidation ($V_i$) were determined at 4 different concentrations.

**c. *In vivo* Study of 64**

Male C57BL/6 mice were housed one per cage in a temperature-controlled room with free access to food and water on a 12 h day/night cycle. Solutions of **64** were prepared in sterile saline at a concentration to provide 0.1 - 0.2 mL injections. Solutions of MPTP·HCl were prepared in sterile saline at a concentration also to provide 0.1 - 0.2 mL injections.

**d. LC-MS Analyses of Standard Compounds and Incubation Mixtures.**

All analyses were performed using an API 365 (Applied Biosystems, Foster City, CA) triple quadrupole tandem mass spectrometer with an electron spray ionization (ESI) source operating in positive mode. The auxiliary gas ($N_2$) flow rate was 2 L/min and

curtain gas 1.3 L/min, 60 psi. The turbo ion spray temperature was 350°C and Mass Chrom 1.2 for MacIntosh software was utilized. The HPLC system was an Agilent 1100 series consisting of a binary pump and UV/Vis diode array detector with a Luna (2 mm x 100 mm, 3 mm) C18 column (Phenomenex). Chromatograms in general were obtained as follows: Selected ion monitoring (identified as XIC in the software) was performed on the parent ion of each compound of interest over a 0.9 amu range in the Q1 quadrant using gradient elution: 0 to 1 min, 100% 20 mM aqueous ammonium formate, 1 to 5 min gradient to 60% $CH_3CN$:40% 20 mM aqueous ammonium formate maintained until 17 min. Chromatograms were smoothed x2. Total ion chromatograms for the incubation mixtures and standard solutions were obtained in the same manner but were recorded over a range of 50-400 amu. Spectra (centroided and averaged over 7 to 15 scans) for the standard compounds were obtained from the relevant total ion chromatograms which, in this case, were obtained using isocratic conditions (mobile phase, 60% $CH_3CN$:40% 20mM aqueous ammonium formate; flow rate, 0.2 mL/min) and recorded over a range of 50-400 amu (Q1 quadrant).

The protocol using animals was approved by the Experimental Animal Care Committee at Virginia Tech.

**Toxicity evaluation**

All injections for the toxicity evaluations were performed by Mrs. Castagnoli. The first injection of **64** was administered at 107 mg/kg. This dose was toxic and a 20% dose was tested next. This subsequent injection was at 21.4 mg/kg. While the two animals receiving this dose did not die, toxicity was observed as the mice did not act normal

after the injections. Next, we tested the dual toxicity of prodrug **64** with MPTP (**2**). To begin with, we performed this test using a 10 % (10.7 mg/kg) dose of **64** and a 35 mg/kg dose of MPTP. This dose resulted in 3 out of 4 mice dying. Finally, 8.025 mg/kg (7.5 % of original dose) of **64** and 30 mg/kg of MPTP (**2**) produced no observed toxicity after the injections.

**Neuroprotective study**

All injections for the neuroprotective study were performed by Mrs. Castagnoli and Dr. Bissel.

**Group 1 (5 mice):** The control group was injected i.v. with sterile saline followed at t = 15 min by sterile saline.

**Group 2 (10 mice):** The MPTP group was injected i.v. with sterile saline followed at t = 15 min by MPTP·HCl (30 mg/kg).

**Group 3 (10 mice):** The MPTP/Prodrug group was injected i.v. with **64** (7.21 mg/kg) followed at t = 15 min by MPTP·HCl (30 mg/kg).

**Group 4 (5 mice):** The Prodrug group was injected i.v. with **64** (7.21 mg/kg) followed at t = 15 min by sterile saline.

On day 7, all mice were sacrificed. Mrs Castagnoli dissected the striata. The mice striata were homogenized and stored at -78°C. On day 9, the striata were analyzed using HPLC/ED. This analysis was similar to that previously used.[55]

[55] Hall, L., Murray, S., Castagnoli, K. and Castagnoli, N. Jr. (1992) Studies on 1,2,3,6-tetrahydropyridine deriviatives as potential monoamine oxidase inactivators. *Chem. Res. Toxicol.* **5**, 625-633.

## VITA

Aaron Downey was born on October 14, 1977 in Norfolk, Virginia. He graduated from Mathews High School in 1995. He finished his Bachelor's of Arts degree in Chemistry in May of 2000. From 2000 – 2004, he worked for Professor James F. Wolfe in the Chemistry department at Virginia Tech. In January 2004, he began his graduate studies under the guidance of Dr. Neal Castagnoli Jr.

He completed his Master's of Science degree in Chemistry in the Fall of 2006. He is currently employed at Scynexis, Inc. in Durham, NC.